

A unified parameterization of clouds and turbulence using CLUBB and subcolumns in the Community Atmosphere Model

Katherine Thayer-Calder^{1,2}, Andrew Gettelman¹, Cheryl Craig¹, Steve Goldhaber¹,
Peter A. Bogenschutz¹, Chih-Chieh Chen¹, Hugh Morrison¹, Jan Höft², Eric Raut²,
Brian M. Griffin², Justin K. Weber², Vincent E. Larson², Matthew C. Wyant³,
Minghuai Wang^{4,5,6}, Zhun Guo⁶, and Steven J. Ghan⁶

¹National Center for Atmospheric Research, Boulder, CO, USA

²University of Wisconsin – Milwaukee, Department of Mathematical Sciences, Milwaukee, WI,
USA

³University of Washington, Department of Atmospheric Sciences, Seattle, WA, USA

⁴Institute for Climate and Global Change Research and School of Atmospheric Sciences, Nanjing
University, Nanjing, 210093, China

⁵Collaborative Innovation Center of Climate Change, Jiangsu Province, China

⁶Pacific Northwest National Laboratory, Richland, WA, USA

Correspondence to: K. Thayer-Calder (katec@ucar.edu)

Abstract.

Most global climate models parameterize separate cloud types using separate parameterizations. This approach has several disadvantages, including obscure interactions between parameterizations and inaccurate triggering of cumulus parameterizations.

- 5 Alternatively, a unified cloud parameterization uses one equation set to represent all cloud types. Such cloud types include stratiform liquid and ice cloud, shallow convective cloud, and deep convective cloud. Vital to the success of a unified parameterization is a general interface between clouds and microphysics. One such interface involves drawing Monte Carlo samples of subgrid variability of temperature, water vapor, cloud liquid, and cloud ice, and feeding the sample points into a
10 microphysics scheme.

- This study evaluates a unified cloud parameterization and a Monte Carlo microphysics interface that has been implemented in the Community Atmosphere Model (CAM) version 5.3. Model computational expense is estimated, and sensitivity to the number of subcolumns is investigated. Results describing the mean climate and tropical variability from global simulations are presented. The new
15 model shows a degradation in precipitation skill but improvements in short-wave cloud forcing, liquid water path, long-wave cloud forcing, precipitable water, and tropical wave simulation.

1 Introduction

Most climate models today use separate parameterizations to model separate cloud types, such as stratiform clouds, shallow cumuli, and deep cumuli. Each parameterization uses its own separate equation set. The resulting suite of parameterizations is intended, collectively, to represent the full range of subgrid-scale clouds included in the climate model.

While the use of separate parameterizations for separate cloud regimes offers several advantages, it also suffers disadvantages. First, the use of multiple, separate cloud parameterizations leads to unnecessary complexity. Some of the complexity is of a practical sort: it is hard to understand a suite of parameterizations written by different authors that use differing coding conventions and assumptions. Some of the complexity is more conceptual in nature: even if each parameterization is simple, the interactions among the parameterizations might be complex (Zhang and Bretherton, 2008; Bretherton, 2007). Second, it is difficult to formulate, in a realistic way, the triggers that are used to activate cumulus parameterizations. For instance, deep convection does not appear instantaneously; rather, in many instances, deep clouds are initiated by the gradual and continuous growth of shallow clouds (Grabowski et al., 2006; Wu et al., 2009). Accurately parameterizing the gradual onset of deep convection is important for modeling tropical phenomena such as the Madden-Julian Oscillation (e.g., Bladé and Hartmann, 1993; Benedict and Randall, 2007; Del Genio et al., 2012; Boyle et al., 2015) and convectively coupled waves (e.g., Lin et al., 2008; Frierson et al., 2011).

To avoid such difficulties, some past researchers have parameterized two or more cloud types using a single equation set, thereby partly unifying the description of clouds. The greater the degree of unification, the greater the reduction in the number of interacting parameterizations and trigger functions.

For instance, to avoid the difficulties of coupling *shallow* and *deep* cumulus parameterizations, some researchers have represented both cloud types using a single parameterization (Kain, 2004; Park, 2014a, b). However, the aforementioned parameterizations are only partly unified because they do not include stratiform clouds; instead, those clouds must be handled by a separate parameterization.

To avoid the difficulties of coupling *stratocumulus* and *shallow cumulus* parameterizations, some researchers have parameterized both cloud types with a single equation set (Lappen and Randall, 2001; Golaz et al., 2002; Larson and Golaz, 2005; Cheng and Xu, 2006, 2008; Firl, 2009; Bogen-schutz and Krueger, 2013). To close some higher-order terms in the equation set, these parameterizations make an assumption about the shape of the probability density function (PDF) of subgrid variability. Assumed PDF parameterizations have a long history in atmospheric science (e.g., Manton and Cotton, 1977; Sommeria and Deardorff, 1977; Mellor, 1977; Bougeault, 1981a, b; Lewellen and Yoh, 1993). For several decades, PDF parameterizations have been implemented in regional or global models (e.g., Smith, 1990; Tompkins, 2002; Nakanishi and Niino, 2004). Recently, the Cloud Layers Unified By Binormals (CLUBB) parameterization has been implemented and evaluated in

two global climate models (Bogenschutz et al., 2013; Guo et al., 2014). In these implementations,
55 CLUBB does unify the representation of boundary layer clouds, but both implementations parameterize deep convection separately. Guo et al. (2015) uses a similar configuration to Guo et al. (2014), but also uses CLUBB to parameterize deep clouds. However, this configuration does not parameterize, in a unified way, subgrid variability in ice clouds.

The configurations used by Bogenschutz et al. (2013), Guo et al. (2014), and Guo et al. (2015)
60 share three drawbacks. First, none of those three configurations fully unifies the description of all cloud variability because in all three configurations, cloud ice is not “seen” by CLUBB. Specifically, cloud ice is not included in CLUBB’s subgrid PDF. Second, even for liquid clouds, the description is, in certain respects, internally inconsistent. For instance, a different marginal PDF shape of cloud water is assumed by CLUBB in order to diagnose cloud liquid water content (namely, a truncated
65 normal mixture) than is assumed by the microphysics in order to compute autoconversion and accretion (namely, a gamma function) (Morrison and Gettelman, 2008). (A univariate marginal PDF is the PDF that remains when a multivariate PDF is integrated over all variates but one.) Third, certain aspects of the subgrid variability, such as the precipitation fraction, are treated by a microphysics scheme that is designed to parameterize stratiform cloud (Morrison and Gettelman, 2008)
70 and whose assumptions about subgrid variability may not be well suited to cumulus clouds. These three drawbacks might be related to certain errors seen in the simulations, such as the overestimate of precipitable water and underestimate of cloud ice noted by Guo et al. (2015).

One key to parameterizing deep convection is accurately parameterizing the subgrid coupling
between clouds and microphysics (Emanuel, 1991; Donner, 1993). The reason is that interactions
75 among condensed water content, clear-air relative humidity, and precipitation evolution are strong. In fact, Hohenegger and Bretherton (2011) state that “the main difference between shallow and deep convection is precipitation (both rain and snow) and its effects.” If true, this hints that a PDF parameterization that can accurately parameterize shallow convection can, in conjunction with a suitable coupling to the microphysics, also parameterize deep convection.

80 Here, in order to interface clouds and microphysics, we use a Monte Carlo integration technique named the Subgrid Importance Latin Hypercube Sampler (“SILHS”) (Larson et al., 2005; Larson and Schanen, 2013). SILHS samples the subgrid PDFs predicted by CLUBB, thereby providing a set of vertical profiles, or “subcolumns,” of sample points. The subcolumns are then fed into a single microphysics scheme, thereby allowing the microphysics to respond to subgrid variability in
85 clouds (Jakob and Klein, 1999; Jess et al., 2011; Tonttila et al., 2013, 2015). Within an individual subcolumn, each grid level has uniform properties (e.g. all cloudy or all clear), but collectively, a set of subcolumns represents the subgrid variability within a grid column. This may improve the representation of non-linear microphysical process rates (Pincus and Klein, 2000; Larson et al., 2001; Jess et al., 2011). Subcolumn approaches have long been used for radiative transfer applications in
90 large-scale models (e.g., Barker et al., 2002; Pincus et al., 2003; Räisänen et al., 2004; Räisänen and

Barker, 2004; Räisänen et al., 2005; Pincus et al., 2006; Räisänen et al., 2007; Barker et al., 2008; Räisänen et al., 2008).

The use of SILHS helps mitigate the three aforementioned drawbacks of the configurations of Bogenschutz et al. (2013), Guo et al. (2014), and Guo et al. (2015). First, cloud ice is included
95 in CLUBB’s subgrid PDF and is sampled by SILHS, thereby driving ice microphysics with subgrid variability. Second, SILHS feeds within-cloud variability directly and consistently into microphysics, ensuring that the same marginal PDF that is used to diagnose cloud water content is also used to diagnose autoconversion. Third, assumptions about subgrid variability, such as those regarding vertical overlap of condensate and vapor, are removed from the microphysics scheme and
100 instead embedded in SILHS (Larson and Schanen, 2013; Storer et al., 2015). This facilitates the implementation of subgrid assumptions that are more general.

Here, we evaluate a new configuration of the CAM climate model that we call “CAM-CLUBB-SILHS.” It shuts off the Zhang and McFarlane (1995) parameterization of deep convection and instead uses CLUBB to parameterize deep cumulus, shallow cumulus, stratiform liquid clouds, and
105 stratiform ice clouds. SILHS is used in order to feed samples of the subgrid variability into a microphysics scheme, following the approach of Storer et al. (2015). A single microphysics scheme is used in all cloud types. This model configuration provides a more fully unified parameterization of clouds. The purpose of the present paper is twofold. First, it outlines the subcolumn software framework in CAM. This software framework contains SILHS. Second, unlike Storer et al. (2015),
110 this paper evaluates the behavior of CLUBB-SILHS in a *global* context, including climatologies of cloud-related fields and some aspects of tropical variability.

This paper is organized as follows. Section 2 describes the CLUBB-SILHS methodology and its implementation in CAM. Section 3 estimates the computational cost of CAM-CLUBB-SILHS. Section 4 evaluates the mean climate versus satellite observations. Section 5 evaluates CAM-CLUBB-SILHS’ simulation of tropical variability. Section 6 illustrates the sensitivity to the number of subcolumns. Section 7 summarizes the evaluation and concludes.

2 Methodology

2.1 Description of the CLUBB moist turbulence parameterization

CLUBB’s methodology is described in Golaz et al. (2002), and an up-to-date listing of CLUBB’s
120 equations is contained in Storer et al. (2015). CLUBB parameterizes subgrid turbulence in both clear and cloudy air, and subgrid variability in all cloud types, including stratiform, shallow cumulus, and deep cumulus.

If CLUBB’s single equation set is to represent turbulence and all cloud types, the equation set must be sufficiently rich and general. CLUBB’s equation set includes prognostic equations for various moments of the vertical air velocity w , the liquid water potential temperature θ_l , and total
125

water mixing ratio (vapor plus liquid cloud water) r_t . The grid-averaged means of these variables are prognosed by the host model, CAM. CLUBB adds prognostic Reynolds-averaged equations for the following moments: $\overline{w'\theta'_l}$, $\overline{w'r'_t}$, $\overline{w'^2}$, $\overline{w'^3}$, $\overline{r'^2_t}$, $\overline{\theta'^2_l}$, $\overline{r'_t\theta'_l}$ (Golaz et al., 2002; Larson and Golaz, 2005). CLUBB parameterizes momentum fluxes using down-gradient diffusion, but CLUBB does
130 not explicitly parameterize subgrid-scale mesoscale convective organization (e.g., Moncrieff, 1992; Donner, 1993; Moncrieff and Liu, 2006).

These prognostic equations include several higher-order moments that are unclosed. To close them, CLUBB integrates them over a PDF of subgrid variability. CLUBB contains a multivariate subgrid PDF for r_t , θ_l , w , cloud ice (mass) mixing ratio r_i , and cloud ice number mixing ratio N_i .
135 The inclusion of r_t and θ_l allows both moisture and temperature fluctuation enter the diagnoses of cloud fraction and cloud water mixing ratio. The inclusion of w allows the buoyancy flux, $\overline{w'\theta'_v}$, to be computed consistently with cloud fraction and cloud water. The inclusion of ice in the PDF allows ice processes to be coupled to the drafts and thermodynamics on the subgrid scale. The marginals of w , r_t , and θ_l are normal mixtures, that is, the sum of two Gaussians. This PDF shape has been shown
140 to compare favorably with aircraft observations and large-eddy simulations of stratiform, shallow cumulus, and deep cumulus clouds (Larson et al., 2002; Bogenschutz et al., 2010). The marginal PDF for r_i and N_i is a delta double-lognormal. That is, the PDF shape for ice is the sum of a delta function representing the ice-free area and the sum of two lognormal distributions. This PDF shape has recently been evaluated against large-eddy simulations (Griffin and Larson, in preparation). The
145 within-ice standard deviation of r_i is assumed to be proportional to the within-cloud mean (Lebo et al., 2015). The same is true for N_i . The correlations among hydrometeors — including mass and number mixing ratios of liquid and ice — are prescribed as in Storer et al. (2015).

2.2 The interface between clouds and microphysics: SILHS

CLUBB computes the transport of hydrometeors and production of cloud water via saturation adjustment, but CLUBB must be coupled to a microphysics scheme in order for other microphysical
150 process rates to be computed. The coupling between clouds and microphysics is accomplished by use of a Monte Carlo sampler called “SILHS”. SILHS’ methodology is described in Larson et al. (2005) and Larson and Schanen (2013). SILHS draws n samples from the subgrid PDF at each grid level. When the liquid cloud fraction is moderate, half the samples are drawn from liquid cloud and
155 half are drawn from the remainder of the grid box, with appropriate weighting, using the method described in Larson and Schanen (2013). The n samples at each grid level are used to construct n vertical profiles of sample points, or subcolumns. In order to parameterize cloud overlap, non-zero vertical correlation between vertical grid levels is allowed. The vertical correlation between samples is assumed to drop off exponentially with vertical distance (Larson and Schanen, 2013).

160 Each subcolumn is fed into Version 1.0 of the Morrison-Gottelman (MG1) microphysics scheme (Morrison and Gottelman, 2008). MG1 provides a simplified initial test for the subcolumn method-

ology because MG1 diagnoses rain and snow. Therefore, rain and snow are not inputs to MG1, and hence the subcolumns need not contain rain or snow variates. In the future, we hope to use SILHS with Version 2.0 of Morrison-Gottelman (MG2) microphysics scheme (Gottelman and Morrison, 2015; Gottelman et al., 2015). MG2 prognoses rain and snow, and hence using it will require us to draw subcolumns with rain and snow. Although this will add complexity and expense, the higher-dimensional PDF will offer greater control over processes that involve two or more hydrometeor species, such as accretion of cloud water by rain water.

When subcolumns are used, MG1’s native assumptions about subgrid variability, including a gamma distribution of cloud water, are shut off, and MG1 is made to assume that each grid level has uniform properties, e.g. is overcast or clear. MG1 calculates time tendencies for cloud ice, cloud liquid water, water vapor, and other relevant microphysical variables. One set of microphysical tendencies is calculated per each subcolumn. The tendencies are then averaged in order to produce a grid-mean tendency. The grid-mean tendencies are then fed into the host model’s grid-mean equations for microphysical species, temperature, and moisture. The averaging is weighted appropriately to account for the fact that different subcolumns may represent different-sized areas of a grid column, as described in Larson and Schanen (2013).

Ice processes are coupled to CLUBB’s grid-mean thermodynamical variables, $\overline{\theta}_l$ and \overline{r}_t , through the microphysics. Subcolumns that include subgrid variability in vapor, liquid, and ice are fed into the microphysics, and the effects of ice, such as the Bergeron effect, are computed by the microphysics at the subgrid scale. These effects of ice are expressed in terms of microphysical tendencies of vapor, liquid, and ice. These tendencies are used to update $\overline{\theta}_l$, \overline{r}_t , and \overline{r}_i . These updated values influence ice during the subsequent time step. In this sense, ice and liquid processes interact on the subgrid scale. Although information about the subgrid PDF of ice is contained within CLUBB, SILHS is needed in order to carry out the subgrid (Monte Carlo) integration of complex, non-linear ice microphysical processes.

Although CLUBB is substepped with a 5-minute time step, MG1 is called with a 30-min (“physics”) time step. At each physics time step, new SILHS sample points are drawn from CLUBB’s PDF from CLUBB’s most recent substep. The subcolumn-averaged microphysical tendencies are fed back into the host model at the end of the physics time step. SILHS retains no memory of sample points from one time step to the next. Rather, the memory is retained within CLUBB’s prognosed moments.

2.3 Comparison of CLUBB-SILHS with other modeling techniques

Now that CLUBB-SILHS’ methodology has been described, we pause and briefly contrast CLUBB-SILHS with other methods.

First, we compare and contrast CLUBB-SILHS with the eddy-diffusivity mass-flux (EDMF) approach (e.g., Soares et al., 2004; Siebesma et al., 2007; Neggers et al., 2009; Neggers, 2009; Sušelj et al., 2012, 2013, 2014). Broadly speaking, two types of grid-box averaging ought to be performed,

explicitly or implicitly, in large-scale models: 1) grid averaging of subgrid turbulent fluxes, and 2) grid averaging of source terms, such as microphysical tendencies. Whereas CLUBB prognoses the turbulent fluxes of moisture and heat content based on the parameterization of each individual term in the flux budget, EDMF diagnoses those turbulent fluxes based on physical considerations. Whereas CLUBB-SILHS averages microphysical tendencies by Monte Carlo integration, EDMF *per se* delegates the averaging of those tendencies to other parameterizations. CLUBB-SILHS is more expensive than EDMF, but CLUBB-SILHS' foundation in PDFs facilitates the consistent calculation of, e.g., cloud fraction and virtual potential temperature, and allows the global use of a single microphysics scheme for all clouds.

Second, we distinguish CLUBB-SILHS from methods that alter the grids on which the equations are solved. We consider two examples of such methods. One is the Multiscale Modeling Framework (MMF, Grabowski (e.g., 2001)). It embeds a convection-permitting model within each grid column of a climate model, thereby unifying the description of cloud features larger than about 4 km in the horizontal extent. Another is the method of Yano et al. (2005), which spectrally decomposes the equations into wavelet modes, and thereby unifies the description of those cloud features that are resolved by the wavelet models. These two methods are more akin to nested gridding or variable-resolution gridding techniques than to parameterizations such as CLUBB. These two methods have the advantage of containing information about the horizontal spatial arrangement of cloud parcels, but they are computationally expensive. For instance, a standard MMF configuration is on the order of 180 times slower than conventional climate models (Khairoutdinov and Randall, 2001).

Finally, we note that CAM-CLUBB-SILHS deviates from common practice in microphysical parameterization. Namely, climate models typically use separate microphysics schemes for separate cloud types, such as stratiform and cumulus clouds. For instance, a relatively sophisticated microphysics scheme might be used in stratiform cloud, and a simpler microphysics scheme might be used in a mass-flux parameterization (e.g., Donner et al., 2011; Neale et al., 2012). In contrast, CAM-CLUBB-SILHS uses a single microphysics scheme, MG1, in all cloud types. Although we have previously mentioned some advantages of using a single, unified parameterization for clouds and turbulence, there are also advantages to using a single, unified scheme for microphysics. For instance, use of a single microphysics scheme avoids complexity and allows aerosol effects on clouds to be parameterized in all cloud types.

2.4 The subcolumn software framework in CAM

The subcolumn software framework in CAM is a newly developed piece of infrastructure that allows subcolumn samplers, such as SILHS, to feed subcolumn values from clouds to microphysics. The subcolumn framework will be available publicly in the release of CAM 5.4 and later versions, and is described in Appendix A.

The call sequence involving subcolumns is as follows:

1. CLUBB calculates a multivariate PDF that contains information about the subgrid variability of temperature, vapor, cloud liquid (mass) mixing ratio, cloud droplet number mixing ratio, cloud ice (mass) mixing ratio, cloud ice number mixing ratio, and vertical velocity.
2. The subcolumn software framework passes information about CLUBB's PDF to the SILHS sampler.
3. SILHS draws subcolumn profiles from CLUBB's PDF. Each subcolumn includes all the aforementioned variates in CLUBB's PDF. The subcolumn framework creates a new model state data-structure with these profiles.
4. Microphysics computes tendencies for all microphysical variates for each subcolumn, on the assumption that each subcolumn is horizontally uniform (e.g., overcast or cloud-free). Aerosol tendencies are not computed on subcolumns.
5. The subcolumn tendencies are averaged together to obtain a grid-mean tendency. This averaging is done by the subcolumn framework using weights provided by SILHS.
6. The grid-mean tendency is applied to the grid-scale values in each column. Energy and water conservation checks are performed.

In order to visualize the flow of the calculations in CAM-CLUBB-SILHS, a schematic is provided in Fig. 1.

In order to ensure conservation of water and energy, the version of CAM-CLUBB-SILHS presented here modifies the sample values such that the weighted mean of all samples is constrained to be the same as the grid-mean value. In the limit of many sample points, the sample mean of the subcolumns converges to the grid mean seen by CLUBB. With a finite number of samples, however, the sample mean will in general differ from the grid mean. If, hypothetically, microphysics were evaluated on a set of samples whose mean exceeded the grid mean, the averaging could produce a mean drying tendency that is larger than the amount of water actually present in the grid column, even though the microphysics guarantees that each subcolumn individually returns non-negative values of water. If this excessive tendency were applied to the grid mean, the resulting negative water would be reset to zero by the energy checker, and a spurious source of water would be created. We prevent this from occurring by scaling the subcolumn values at each level and each time step by a constant factor, so that the weighted mean of the subcolumns exactly matches the grid-mean value at that point. The scaling occurs after SILHS has drawn sample values but before those values have been fed into the microphysics. This scaling has the undesirable side effect of effectively reducing the standard deviation of the subgrid PDFs. However, CLUBB's assumption that the standard deviation is proportional to the mean has uncertainty regardless of whether any scaling is done. Other than this scaling, no upper limit is placed on the values of the samples. We constrain the means of water

vapor, liquid and ice mass mixing ratio, and liquid and ice number mixing ratio, but not temperature and vertical velocity.

270 2.5 Configuration of CAM simulations

All of the CAM-CLUBB-SILHS simulations presented here are based on the CAM 5.3 model code with the addition of the subcolumn framework. Our code branched from the CAM development trunk at tag 5_3_38. We use CLUBB and SILHS revision 7508 in these simulations. The simulations presented here are uncoupled atmosphere-only runs, using prescribed climatological sea surface temperatures as a data ocean (CESM component set F_2000). Unless otherwise stated, all of our simulations use 2-degree resolution, 30 vertical grid levels, and 10 subcolumns. All of our simulations use the Finite Volume dynamical core and an 1800-second physics time step. None of the CAM-CLUBB-SILHS simulations uses the Zhang and McFarlane (1995) deep convection scheme. Table 1 details the differences in physical parameterizations between CAM 5.3 and CAM-CLUBB-SILHS. The model code used in these simulations is stored within the CAM development repository and is available upon registration and request from the corresponding author. Results in this paper are based on tag subcol16_SILHS_cam5_3_38, which is not a publicly released version of CAM. CLUBB and SILHS source code is publicly available at http://clubb.larson_group.com.

3 Computational cost

285 Simulations were performed on the Yellowstone supercomputer administered by the National Center for Atmospheric Research (NCAR) (Computational and Information Systems Laboratory, 2015). Estimates of the computational cost of running different configurations of CAM-CLUBB-SILHS are shown in Table 2. A configuration without subcolumns but with CLUBB handling all convection is about 63% more expensive than basic CAM 5.3 in terms of total wall clock time. Using 4 subcolumns increases the cost another 25%, and using 10 subcolumns adds 57%. This implies a cost of about 6% per subcolumn.

It is currently unknown how much the cost per subcolumn can be reduced by optimization. Another way to reduce the cost is to draw more representative subcolumns, so that fewer subcolumns are needed. In the future, we will evaluate a new sampling method that produces equal accuracy with about half as many subcolumns (Raut and Larson, 2015).

These test runs for timing do not attempt to vectorize subcolumn calculations. Since subcolumns do not communicate with each other, they can be efficiently parallelized. For this reason, subcolumn-based methodologies are well suited to take advantage of vector processing and the next generation of high-performance computers.

300 4 Mean climate

This section evaluates the time-averaged climatology simulated by CAM-CLUBB-SILHS. We compare three versions of CAM — CAM-CLUBB-SILHS with 2-degree horizontal resolution, CAM-CLUBB-SILHS with 1-degree horizontal resolution, and CAM 5.3 with 2-degree horizontal resolution — to a range of observational datasets that are summarized in Table 3. More information on each
305 observational field, including specific references and discussion of observational uncertainties, can be found online with the National Center for Atmospheric Research (NCAR) Climate Data Guide at <https://climatedataguide.ucar.edu/>. In all figures in this section, the first row of plots shows the total field, and the second row shows differences from observations (model - obs).

Total surface precipitation rates for the three model versions and the Global Precipitation Climatology Project (GPCP) observations are presented in Fig. 2. CAM 5.3 exhibits a moderate, spurious
310 double Inter-Tropical Convergence Zone (ITCZ), that is, a double band of precipitation in the Indian Ocean, and, to a lesser extent, in the Equatorial Pacific. Both versions of CAM-CLUBB-SILHS produce a single band of rain through the tropics, thereby reducing the double-ITCZ bias. However, CAM-CLUBB-SILHS' precipitation is too intense and its ITCZ is too narrow, as compared to
315 GPCP observations. The overall pattern of precipitation is similar between the 2-degree and 1-degree simulations, but the RMSE increases in the 1-degree simulation due to noise in the rain rate field.

CAM-CLUBB-SILHS slightly improves the mean climatological column-integrated water vapor (Fig. 3), as compared to NVAP observations. CAM 5.3's overestimate of precipitable water is reduced in both the CAM-CLUBB-SILHS 2-degree and 1-degree simulations. The 2-degree and 1-
320 degree simulations resemble each other, with the 1-degree simulation providing a closer match to observations. Furthermore, the bias in precipitable water for the 1-degree simulation is reduced by a factor of 4 as compared to the results of Guo et al. (2015). The improvement may be related to the fact that SILHS contains a detailed representation of hydrometeor/vapor overlap (Larson and Schanen, 2013; Storer et al., 2015), which influences the evaporation or accretional growth of precipitation as
325 it falls to the ground or ocean (Jakob and Klein, 1999).

The top-of-the-atmosphere (TOA) long-wave cloud forcing (LWCF) for the three models is compared to observations in Fig. 4. Both versions of CAM-CLUBB-SILHS have smaller bias and lower RMSE in LWCF than does CAM 5.3. Furthermore, CAM-CLUBB-SILHS' bias is about a factor
330 of 4 less than that of the simulation of Guo et al. (2015). The representation of LWCF in CAM-CLUBB-SILHS is aided by the fact that SILHS samples within-cloud variability of ice and feeds it into the microphysics scheme. Within-cloud subgrid-scale variability in ice is important because several ice processes are non-linear (Morrison and Gettelman, 2008).

The use of CLUBB-SILHS improves the TOA short-wave cloud forcing (SWCF) (Fig. 5). CAM 5.3 produces excessively reflective clouds over tropical land masses, probably because the deep con-
335 vective microphysics does not precipitate out sufficient liquid cloud water. Use of CAM-CLUBB-SILHS, however, mitigates the excessive reflectivity of deep cumuli. The improvement may be re-

lated to the fact that accurate parameterization of the SWCF of deep cumuli requires accurate coupling of subgrid variability of clouds and precipitation (which in CAM-CLUBB-SILHS is handled by SILHS) and also requires accurate parameterization of deep convective microphysics itself (which in CAM-CLUBB-SILHS is handled by MG1).

The total grid-box cloud fraction for the three models and observations is presented in Fig. 6. Both versions of CAM-CLUBB-SILHS have a slightly lower cloud fraction (by about 5%) than do CAM 5.3 or the observations. This is largely due to a lower cloud fraction throughout the tropics and subtropics in CAM-CLUBB-SILHS.

CAM-CLUBB-SILHS has about 35% more total grid-mean liquid water path (LWP) than does CAM 5.3, improving the agreement with observations (Fig. 7). It is notable that CAM-CLUBB-SILHS improves (increases) LWP without degrading (increasing the magnitude of) SWCF. How do the clouds in CAM-CLUBB-SILHS increase in water mass without increasing in reflectivity? A first reason is that CAM-CLUBB-SILHS' cloud fraction is slightly decreased in the Tropics, as noted earlier. The decrease in cloud fraction, coupled with the increase in LWP, indicates that within-cloud cloud liquid water is increased in CAM-CLUBB-SILHS, either because the cloud liquid water has a more adiabatic profile, is more vertically stacked, or is more temporally intermittent. This "piled-up" vertical structure of LWP allows more solar radiation to reach the ocean or land surface (not shown) and thereby leads to reduced cloud reflectivity per unit of LWP. A second reason is that CAM-CLUBB-SILHS' cloud droplet effective radius is increased (not shown), thereby decreasing the reflectivity per unit of within-cloud LWP. Accurate simulation of droplet radius in deep convection requires accurate formulation of microphysics, which in CAM-CLUBB-SILHS is handled by the MG1 microphysics.

Figure 8 shows the Taylor Score diagram for CAM 3.5, CAM 5.3, and 2-degree CAM-CLUBB-SILHS (Taylor, 2001). CAM-CLUBB-SILHS is competitive with CAM 5.3 on most metrics, but has a higher RMSE in land rainfall, ocean rainfall, and the Pacific surface stress. The fact that Pacific surface stress is degraded suggests that CLUBB's formulation of vertical momentum flux, which is based on downgradient diffusion, needs to be modified in future work.

Table 4 shows the top of the atmosphere (TOA) global mean values for several radiation and energy balance terms, with mean values calculated from the observational datasets described in Table 3 and estimated uncertainties from Stephens et al. (2012). Unlike CAM 5.3, CAM-CLUBB-SILHS has not yet been tuned for top of model (TOM) radiative balance. Such tuning will be necessary before coupled simulations are attempted.

The differences between CAM-CLUBB-SILHS at 2-degree or 1-degree horizontal resolution are minor in the both globally averaged radiation (Table 4) and in the spatial patterns of radiation and cloud fields (Figs. 3 to 8). This suggests that CAM-CLUBB-SILHS is relatively insensitive to small changes in horizontal resolution, aside from localized phenomena such as near-coastal marine stratocumulus clouds. In CAM-CLUBB-SILHS, the treatment of subgrid variability is removed from

the microphysics and handled instead by CLUBB and SILHS. This removes one potential source of
375 sensitivity to grid scale.

5 MJO and tropical variability

The outgoing longwave radiation (OLR) power divided by the background spectrum for various
zonal wave numbers and frequency (as in Wheeler and Kiladis (1999) Fig. 3b) is shown in Fig. 9 for
CAM 5.3, CAM-CLUBB-SILHS, and observations. This figure shows that, as compared to CAM
380 5.3, CAM-CLUBB-SILHS has increased power in the low-wavenumber, low-frequency, eastward-
propagating region of the spectrum associated with the Madden Julian Oscillation (MJO). The MJO
power is not as strong as in the observations, and the frequency is slightly too high. The power
associated with Kelvin waves is also increased in CAM-CLUBB-SILHS as compared to CAM 5.3,
and compares well to the observations. However, CAM-CLUBB-SILHS has too much power in the
385 high-frequency, westward-propagating side of the spectrum often associated with large convective
systems advected westward by the mean flow (Wheeler and Kiladis, 1999).

Figure 10 shows the 20-80 day bandpass filtered precipitation and U 850 hPa winds at a given
lag relative to a composite MJO passage and at a given Longitude (top) and Latitude (bottom). The
MJO precipitation for CAM-CLUBB-SILHS is weaker than both the observations and CAM 5.3, but
390 shows eastward propagation at the correct phase and speed. The overall coherence and structure of
the MJO is much better in CAM-CLUBB-SILHS than in CAM 5.3. Figure 10 indicates that CAM
5.3 has primarily westward propagation of disturbances at this scale and has westerly winds nearly
in phase with the maximum in precipitation. In contrast, CAM-CLUBB-SILHS simulates eastward
propagation, with eastward winds leading the precipitation and westward winds following, as seen
395 in the observations.

In order to investigate differences in tropical convective processes between CAM 5.3 and CAM-
CLUBB-SILHS, Fig. 11 shows average profiles of relative humidity, total physics moisture tendency
and total physics temperature tendencies per value of rain rate for latitudes between 15 north and 15
south and longitudes between 60 east and 180 east (the Indian Ocean and West Pacific Warm Pool).
400 These are similar to diagnostics used to evaluate MJO fidelity in Thayer-Calder and Randall (2009),
Kim et al. (2009), Xavier (2012), and Kim et al. (2014). All of these studies stress the importance
of a smooth, gradual build-up in moisture from shallow convection (and light precipitation) to deep
convection (and intense precipitation).

In observations, and in most models with a realistic MJO simulation, deep convection occurs in
405 a nearly saturated column (Bretherton et al., 2004; Kim et al., 2009; Halloway and Neelin, 2009).
Figure 11 shows that CAM 5.3 does not produce rain rates as intense as those simulated in CAM-
CLUBB-SILHS; thus the right-most profiles are missing. However, both models have nearly sat-
urated profiles for the most intense rain rates that do occur. CAM-CLUBB-SILHS has a deeper

boundary layer with higher relative humidity for mid-range precipitation values (between 0.5 and
 410 10 mm day⁻¹) than CAM 5.3. The relative humidity contours also show a smoother transition be-
 tween light and intense precipitation than CAM 5.3. The transition from 80% relative humidity in
 the boundary layer to near saturation around 11 mm day⁻¹ in CAM 5.3 is more abrupt than reanal-
 ysis shown in similar results from Kim et al. (2009) Fig. 13 and Xavier (2012) Fig. 3. This abrupt
 transition may be an ill effect of poor deep convection triggering function. In contrast, the unified
 415 convection in CAM-CLUBB-SILHS produces a smooth deepening of the boundary layer into a fully
 saturated column at high rain rates.

Figure 11 also shows the total physics moisture and temperature tendencies for both models.
 CAM-CLUBB-SILHS shows strong moistening in shallow convective layers that transitions smoothly
 to intense drying through the entire column for deep convection. Similarly, the temperature ten-
 420 dencies smoothly change from low level heating, to convection rising in depth, to intense heating
 through nearly the entire column. These profiles resemble results for the SP-CAM presented in
 Thayer-Calder and Randall (2009) Figs. 4 and 9. The SP-CAM has been shown to simulate a realis-
 tic MJO (Khairoutdinov et al., 2008; Benedict and Randall, 2009), and so producing similar results
 in these diagnostics is promising.

In contrast, CAM 5.3 seems to have two main regimes. In the first, shallow convection produces
 light moistening tendencies above and below a layer of cloud-related drying around 900 hPa. This
 cloud layer produces a positive temperature tendency above a layer of cooling for all precipitation
 rates between 0.0003 mm day⁻¹ and 2.5 mm day⁻¹. Past this point, there is an abrupt transition to con-
 vective drying and warming below 700 hPa, and then to a full column of drying above about 30 mm
 430 day⁻¹. However, unlike CAM-CLUBB-SILHS, the most intense precipitation in CAM 5.3 has strong
 heating only above 600hPa. Again, the transition in moistening and heating rates is more abrupt than
 that seen in similar plots by Thayer-Calder and Randall (2009). There is a clear signal in CAM 5.3
 of an unrealistic transition from convection handled by the shallow/stratiform parameterizations to
 convection produced by the Zhang and McFarlane (1995) deep convection parameterization.

There are still deficiencies in the simulation of the MJO by CAM-CLUBB-SILHS, but our unified
 parameterization of clouds produces promising improvements in the build-up of tropical moisture
 and the transition from shallow to deep convection. Boyle et al. (2015) show that an acceptable MJO
 in CAM 5.3 can be produced with tuning changes, but only at the expense of the mean climate.
 Our structural changes to CAM 5.3 have, in one and the same simulation, produced a realistic mean
 440 climate and improved tropical variability.

6 Subcolumn impact

In order to evaluate the impact of the number of subcolumns on these simulations, we performed
 four sensitivity experiments. All four simulations use the exact same settings and tuning parameters

as the main 20-year, 2-degree simulation described in Sect. 2.5. In our *No Subcolumns* simulation,
 445 we turned off the subcolumn sampler (SILHS), fed CLUBB’s cloud fraction into MG1 microphysics,
 and enabled MG1’s assumptions about subgrid variability that are operative in CAM5.3, including
 a subgrid integration over cloud liquid water. The deep convection parameterization remains turned
 off here. This simulation indicates how CAM5.3 would behave if it used CLUBB as a unified pa-
 rameterization and it used MG1’s subgrid assumptions, developed for stratiform clouds. The three
 450 other simulations varied the number of subcolumns from 4 to 10 to 50. Because of restrictions in
 the SILHS importance sampling algorithm (Larson and Schanen, 2013), the number of subcolumns
 must always be divisible by two.

As expected, the simulation without subcolumns produces an unrealistic climate. Figure 12 shows
 that the *No Subcolumns* simulation has very low longwave cloud forcing, and Table 4 shows this
 455 simulation has the highest OLR, largest radiative imbalance, and greatest error in SWCF. This is
 likely because the convection is not penetrating as deeply into the atmosphere, and the clouds are
 not cold and icy enough. This is supported by the large shortwave cloud forcing for the simulation
 (Table 4), which has a high bias and RMSE in Fig. 13. Figure 14 shows that this simulation has an
 even lower LWP than that of CAM 5.3.

The simulation with only four subcolumns shows marked improvement over the *No Subcolumns*
 simulation. Table 4 shows a large decrease in both net solar TOA flux and OLR, with reasonable
 values of LWCF, but a lower SWCF corresponding to brighter clouds. This is also seen in Fig. 13,
 where the low bias in SWCF is distributed over all oceans. This low bias in SWCF is tied to the
 higher cloud LWP for this simulation (Fig. 14). The 4-subcolumn simulation appears to have a lower
 465 precipitation efficiency than the 10-subcolumn simulation. The reason, we speculate, is that use of a
 limited number of subcolumns leads to poor sampling of the tails of the distribution, which is where
 precipitation forms and grows.

The 10- and 50-subcolumn simulations are similar, suggesting that climatological averages are
 fairly close to converged even when only 10 subcolumns are used. Table 4 shows that increasing to
 470 50 subcolumns decreases the OLR by 1 W m^{-2} and increases the net Solar flux by 0.5 W m^{-2} . Figure
 12 shows that the LWCF is very similar between the 10- and 50-subcolumn runs. Both simulations
 have similar SWCF (Fig. 13) and LWP (Fig. 14). The fact that LWP decreases when the number of
 subcolumns is increased to 50 supports the hypothesis that increasing subcolumns increases precip-
 itation efficiency, although there is diminishing effect after 10 subcolumns.

475 7 Summary and Conclusions

This paper evaluates a version of CAM, “CAM-CLUBB-SILHS”, that uses a single equation set to
 parameterize all cloud types, including shallow convective, deep convective, and stratiform liquid
 and ice clouds. The equation set is CLUBB’s set of equations for higher-order moments. CLUBB

uses the higher-order moments to construct a multivariate subgrid PDF, which, in turn, is sampled
480 by SILHS. The samples are then used to drive a single microphysics scheme, MG1, that acts on all
cloud types. In CAM-CLUBB-SILHS, clouds are parameterized in a more fully unified way, and so
are microphysical processes.

The use of a single, multivariate subgrid PDF fosters consistency in the sense that all cloud and
microphysical processes see the same subgrid PDF. In this paper, the PDF has been extended to
485 include cloud ice mass and number, thereby incorporating subgrid variability in ice processes.

As compared to CAM5, the most important degradation in the CAM-CLUBB-SILHS simulations
is the root-mean-square error in surface precipitation rate. In particular, the surface precipitation field
is stronger in the precipitating regions than that observed by satellite. However, several aspects of
the simulations have been improved. We list the improvements here, even though it is difficult to
490 pinpoint their causes.

First, CLUBB-SILHS slightly reduces CAM5's overestimate of precipitable water. This may be
related to the fact that CLUBB-SILHS contains a detailed representation of vertical overlap, which
affects the relative rates of evaporation and accretional growth of precipitation.

Second, CLUBB-SILHS improves LWCF. In general, CLUBB-SILHS offers a more detailed rep-
495 resentation of subgrid variability in ice because cloud ice mass and number mixing ratio are included
in the subgrid PDF. The inclusion of ice in the PDF, in turn, allows subgrid variability in ice to drive
ice-related microphysical processes.

Third, CLUBB-SILHS simultaneously improves the simulation of both LWP and SWCF. In CAM5,
LWP is underestimated by almost a factor of 2, and deep convective clouds are too reflective over the
500 tropical continents. In CAM-CLUBB-SILHS, LWP is increased without unduly increasing the mag-
nitude of SWCF. In part, this is related to the fact that CAM-CLUBB-SILHS predicts smaller cloud
fraction. That is, CAM-CLUBB-SILHS' liquid water content is more vertically and/or temporally
correlated and less horizontally extended, allowing more LWP to be present without causing exces-
sive cloud albedo. In addition, in CAM-CLUBB-SILHS, the cloud liquid droplet radius is increased,
505 thereby reducing reflectivity of clouds.

Fourth, although CLUBB-SILHS underestimates MJO wave activity, it improves (strengthens) the
spectral power associated with the MJO and convectively coupled Kelvin waves. The improvement
may be related to the fact that CLUBB-SILHS is a unified parameterization in which there is no
categorization of clouds nor a cumulus trigger function. This allows for a smoother, more realistic
510 transition between shallow and deep convection in the tropics.

The simultaneous improvement of LWP, SWCF, and tropical power spectrum is significant. Use of
automated parameter estimation reveals that although CAM5's MJO can be improved by changes in
parameter values, the improvement comes at the expense of the simulated climatology, including the
absorption of short-wave radiation (Boyle et al., 2015). This suggests that, in order to simultaneously

515 improve CAM 5.3's MJO and mean state, structural modifications to the parameterization suite are required. The use of CLUBB-SILHS is one possible structural modification.

The results are relatively insensitive to an increase in resolution from 2° to 1° . Avoiding undesirable grid-scale sensitivity is aided by the fact that CAM-CLUBB-SILHS does not require the microphysics scheme to internally account for resolution changes. Instead, any model awareness of
520 horizontal resolution is contained in CLUBB and is communicated to the microphysics via SILHS. As cloud-resolving resolutions are approached, CLUBB is designed to gradually shut itself off by reducing its turbulent dissipation time scale (Larson et al., 2012). Whether in practice the output of CAM-CLUBB-SILHS proves to be sensitive to significant changes in resolution is left for future work.

525 Although acceptable results can be found with as few as four sample points per grid box and physics time step, the results are moderately sensitive to the number of sample points. This suggests that climate simulations are sensitive to the details of subgrid variability within clouds and how such variability is communicated to the microphysics. Therefore, it is worth investigating subgrid integration methods, whether they be Monte Carlo methods or alternative methods. One alternative method
530 is analytic integration, which is computationally inexpensive but is restricted to simple microphysical formulations (Morrison and Gettelman, 2008; Larson and Griffin, 2013; Griffin and Larson, 2013). Another alternative method is deterministic quadrature, which requires somewhat intrusive software changes but is more generally applicable than analytic integration (Golaz et al., 2011; Chowdhary et al., 2015).

535 Each subcolumn that is added increases the total model computational cost by about 6%. This cost is reasonable, considering the wealth of detail that is output by subcolumns.

Much further unification of parameterizations of subgrid variability is possible in the future. Although CLUBB-SILHS unifies the parameterization of subgrid-scale variability in clouds and feeds that information into a microphysics scheme, that information is not fed consistently into aerosol,
540 radiative, or land surface processes. That extension is left for future work.

Appendix A: CAM subcolumn implementation

A1 Description of subcolumn implementation

Subcolumns were implemented in CAM to assist in the study of subgrid-scale physics. The implementation supports both studies based on spatial subdivision of a physics column and studies based
545 on statistical sampling of subgrid variability (e.g., SILHS). Other features of the CAM implementation of subcolumns are:

- Use subcolumns to study subgrid-scale physics in a select subset of physics parameterizations.

- Subcolumn data may be shared between parameterizations (for example, passing microphysics subcolumns to the radiative transfer scheme).
- 550 – The subcolumn scheme (see below) may specify a different number of subcolumns per grid column (e.g., 15 subcolumns per grid column in the tropics, 2 elsewhere).
- The memory layout provides for efficient, threaded performance and seamless use in current, portable code layers (see Fig. A1).
- Subcolumn data may persist across time steps.
- 555 – If subcolumns are not invoked, the basic model state is not altered.
- Parameterizations themselves do not need to know about subcolumns because information is passed at the interface and driver levels.
- Subcolumn information can be output for analysis.

Subcolumns in CAM are considered static: once the number of subcolumns in any grid column is set at the beginning of simulation, this number should not be changed. The subcolumn framework supports only instantaneous history output of subcolumn fields. Currently, the only CAM physics parameterization that accepts subcolumn input is the Morrison-Gettelman microphysics (Morrison and Gettelman (2008)). However, the software framework allows subcolumns to be applied to other parameterizations. A key goal is to apply subcolumns uniformly across the column physics: for example, currently there are separate subcolumn generators for radiation and satellite simulators in CAM, these could be made consistent with this framework.

Use of subcolumns begins with sampling or generation of subgrid fields based on the current physics state. In this way, a complete state on subcolumns is passed to the parameterization. The sampling can occur by any method (in this case SILHS) and for arbitrary fields. Parameterizations then use these fields to produce subgrid tendencies. Finally, the subgrid state and tendencies are averaged back to the grid scale. The subcolumn “gather” or averaging routines can be customized so that averaging can be performed using weights or masking if desired. Organization of different methods for drawing or generating subcolumns and averaging them back to the grid is described below. For more details or for documentation on making a parameterization subcolumn aware, see the CAM reference manual (Eaton et al. (2015)).

A2 Implementing a new subcolumn scheme within CAM

Different methods or “schemes” for generating and averaging subcolumn fields can be invoked. SILHS is one subcolumn scheme. The use of a specific subcolumn scheme is controlled by the CAM `subcol_scheme` namelist variable. Each of the generic subcolumn interfaces listed below call the scheme-specific version based on the value of `subcol_scheme`. Scheme-specific versions

of the following routines will need to be supplied, even if they contain no executable code. Typically the scheme-specific versions are designated by the generic name followed by “_schemeName”, noted below by XXX (e.g., `subcol_register_SILHS`). The routines are:

`subcol_register_XXX`: Register any subcolumn-specific physics buffer fields using `pbuf_add_field`.

585 `subcol_readnl_XXX`: Read any subcolumn-scheme-specific namelist parameters.

`subcol_init_XXX`: Perform subcolumn-specific initialization, set up any output calls for subcolumn diagnostics (via `addfld`), and initialize any subcolumn physics buffer fields, if required.

590 `subcol_gen_XXX`: Contains the details of mapping state, physics tendencies, and physics buffer fields from the grid to subcolumns. Typically, this routine will be the interface between CAM and the unique code for generating the subcolumns or drawing them from PDFs.

Once physics tendencies and/or updates are computed for each subcolumn, the subcolumn values need to be averaged back onto the CAM grid. This is accomplished via calls to averaging routines. The default behavior of these routines is to perform a simple average, applying optionally supplied

595 scheme-specific weights and/or filters, such as a cloud mask or conditional sampler. If a more sophisticated method is required, scheme-specific routines may be supplied for these two routines.

`subcol_ptend_avg_XXX`: Average the subcolumn physics tendency values back to the grid so that these values can be applied to the grid-resolved state.

600 `subcol_field_avg_XXX`: Average the physics buffer fields from subcolumn values back to the grid. This function only needs to be called for physics buffer fields which are used in other parameterizations on the grid.

The data layout for subcolumns is illustrated in Fig. A1. The number of subcolumns varies by grid column, as shown in the conceptual layout (Fig. A1, left). Internally, the subcolumns are stored in a compressed layout (Fig. A1 right). The information on organization is stored in a series of

605 parameters some of which can be set by the user (black) and others which are internally calculated (blue). For further details, see Eaton et al. (2015).

Acknowledgements. The National Center for Atmospheric Research is supported by the U.S. National Science Foundation. NCAR authors were partially supported by National Science Foundation Grant AGS-0968657. Co-authors from University of Wisconsin — Milwaukee acknowledge support by the Office of Science, U. S.

610 Department of Energy, under grants DE-SC0008668 (BER) and DE-SC0008323 (Scientific Discoveries through Advanced Computing, SciDAC) and support by the National Science Foundation under grant AGS-0968640. PNNL staff were supported by SciDAC and the DOE Atmospheric System Research (ASR) Program. The Pacific Northwest National Laboratory is operated for DOE by Battelle Memorial Institute under contract DE-AC06-76RLO 1830.

615 References

- Barker, H. W., Pincus, R., and Morcrette, J.-J.: The Monte Carlo Independent Column Approximation: Application within large-scale models, in: Proceedings of the GCSS workshop, Kananaskis, Alberta, Canada, Amer. Meteor. Soc., 2002.
- Barker, H. W., Cole, J. N. S., Morcrette, J.-J., Pincus, R., Räisänen, P., von Salzen, K., and Vaillancourt, P. A.:
620 The Monte Carlo Independent Column Approximation: An Assessment using Several Global Atmospheric Models, *Quart. J. Roy. Meteor. Soc.*, 134, 1463–1478, 2008.
- Benedict, J. J. and Randall, D. A.: Observed characteristics of the MJO relative to maximum rainfall, *J. Atmos. Sci.*, 64, 2332–2354, 2007.
- Benedict, J. J. and Randall, D. A.: Structure of the Madden-Julian oscillation in the superparameterized CAM,
625 *J. Atmos. Sci.*, 66, 3277–3296, 2009.
- Bladé, I. and Hartmann, D. L.: Tropical intraseasonal oscillations in a simple nonlinear model, *Journal of the atmospheric sciences*, 50, 2922–2939, 1993.
- Bogenschutz, P. A. and Krueger, S. K.: A simplified PDF parameterization of subgrid-scale clouds and turbulence for cloud-resolving models, *J. Adv. Model. Earth Syst.*, 5, doi:10.1002/jame.20018, 2013.
- 630 Bogenschutz, P. A., Krueger, S. K., and Khairoutdinov, M.: Assumed Probability Density Functions for Shallow and Deep Convection, *J. Adv. Model. Earth Syst.*, 2, doi:10.3894/JAMES.2010.2.10, 2010.
- Bogenschutz, P. A., Gettelman, A., Morrison, H., Larson, V. E., Craig, C., and Schanen, D. P.: Higher-Order Turbulence Closure and Its Impact on Climate Simulations in the Community Atmosphere Model, *J. Climate*, 26, 9655–9676, doi:10.1175/JCLID-13-00075.1, 2013.
- 635 Bougeault, P.: Modeling the trade-wind cumulus boundary layer. Part I: Testing the ensemble cloud relations against numerical data, *J. Atmos. Sci.*, 38, 2414–2428, 1981a.
- Bougeault, P.: Modeling the trade-wind cumulus boundary layer. Part II: A higher-order one-dimensional model, *J. Atmos. Sci.*, 38, 2429–2439, 1981b.
- Boyle, J. S., Klein, S. A., Lucas, D. D., Ma, H.-Y., Tannahill, J., and Xie, S.: The parametric sensitivity of CAM5's MJO, *Journal of Geophysical Research: Atmospheres*, 120, 1424–1444, doi:10.1002/2014JD022507, 2014JD022507, 2015.
- 640 Bretherton, C., Peters, M. E., and Back, L. E.: Relationships between water vapor path and precipitation over the tropical oceans, *J. Climate*, 17, 1517–1528, 2004.
- Bretherton, C. S.: Challenges in Numerical Modeling of Tropical Circulations, in: *The Global Circulation of the Atmosphere*, edited by Schneider, T. and Sobel, A. H., pp. 302 – 330, Princeton University Press, 2007.
- 645 Bretherton, C. S. and Park, S.: A New Moist Turbulence Parameterization in the Community Atmosphere Model, *J. Climate*, 22, 3422–3448, 2009.
- Cheng, A. and Xu, K.-M.: Simulation of shallow cumuli and their transition to deep convective clouds by cloud-resolving models with different third-order turbulence closures, *Quart. J. Roy. Meteor. Soc.*, 132, 359–382,
650 2006.
- Cheng, A. and Xu, K.-M.: Simulation of Boundary-Layer Cumulus and Stratocumulus Clouds Using a Cloud-Resolving Model with Low- and Third-order Turbulence Closures, *J. Meteor. Soc. Japan*, 86A, 67–86, 2008.
- Chowdhary, K., Salloum, M., Debusschere, B., and Larson, V. E.: Quadrature methods for the calculation of subgrid microphysical moments, *Mon. Wea. Rev.*, 143, 2955–2972, 2015.

- 655 Computational and Information Systems Laboratory: Yellowstone: IBM iDataPlex System (University Community Computing). Boulder, CO: National Center for Atmospheric Research. <http://n2t.net/ark:/85065/d7wd3xhc>, 2015.
- Del Genio, A. D., Chen, Y., Kim, D., and Yao, M.-S.: The MJO transition from shallow to deep convection in CloudSat/CALIPSO data and GISS GCM simulations, *J. Climate*, 25, 3755–3770, 2012.
- 660 Donner, L. J.: A cumulus parameterization including mass fluxes, vertical momentum dynamics, and mesoscale effects, *J. Atmos. Sci.*, 50, 889–906, 1993.
- Donner, L. J., Wyman, B. L., Hemler, R. S., Horowitz, L. W., Ming, Y., Zhao, M., Golaz, J.-C., Ginoux, P., Lin, S.-J., Schwarzkopf, M. D., et al.: The Dynamical Core, Physical Parameterizations, and Basic Simulation Characteristics of the Atmospheric Component AM3 of the GFDL Global Coupled Model CM3., *Journal of*
- 665 *Climate*, 24, 3484–3519, 2011.
- Eaton, B., Goldhaber, S., and Craig, C.: CAM Reference Manual, http://www.cesm.ucar.edu/models/cesm1.3/cam/docs/rm5_4, 2015.
- Emanuel, K. A.: A scheme for representing cumulus convection in large-scale models, *J. Atmos. Sci.*, 48, 2313–2329, 1991.
- 670 Firl, G.: Development of a Second-Order Closure Turbulence Model with Subgrid-Scale Condensation and Microphysics, M.S. Thesis, Colorado State University, Fort Collins, CO, 2009.
- Frierson, D. M., Kim, D., Kang, I.-S., Lee, M.-I., and Lin, J.: Structure of AGCM-simulated convectively coupled Kelvin waves and sensitivity to convective parameterization, *J. Atmos. Sci.*, 68, 26–45, 2011.
- Gettelman, A. and Morrison, H.: Advanced Two-Moment Bulk Microphysics for Global Mod-
- 675 els. Part I: Off-Line Tests and Comparison with Other Schemes, *J. Climate*, 28, 1268–1287, doi:<http://dx.doi.org/10.1175/JCLI-D-14-00102.1>, 2015.
- Gettelman, A., Morrison, H., Santos, S., Bogenschutz, P., and Caldwell, P. M.: Advanced Two-Moment Bulk Microphysics for Global Models. Part II: Global model solutions and Aerosol-Cloud Interactions, *J. Climate*, 28, 1288–1307, doi:<http://dx.doi.org/10.1175/JCLI-D-14-00103.1>, 2015.
- 680 Golaz, J.-C., Larson, V. E., and Cotton, W. R.: A PDF-based model for boundary layer clouds. Part I: Method and model description, *J. Atmos. Sci.*, 59, 3540–3551, 2002.
- Golaz, J.-C., Salzmann, M., Donner, L. J., Horowitz, L. W., Ming, Y., and Zhao, M.: Sensitivity of the aerosol indirect effect to subgrid variability in the cloud parameterization of the GFDL Atmosphere General Circulation Model AM3, *Journal of Climate*, 24, 3145–3160, doi:10.1175/2010JCLI3945.1, 2011.
- 685 Grabowski, W. W.: Coupling cloud processes with the large-scale dynamics using the cloud-resolving convection parameterization (CRCP), *J. Atmos. Sci.*, 58, 978–997, 2001.
- Grabowski, W. W., Bechtold, P., Cheng, A., Forbes, R., Halliwell, C., Khairoutdinov, M., Lang, S., Nasuno, T., Petch, J., Tao, W. K., Wong, R., Wu, X., and Xu, K. M.: Daytime convective development over land: A model intercomparison based on LBA observations, *Quart. J. Roy. Meteor. Soc.*, 132, 317–344, 2006.
- 690 Griffin, B. M. and Larson, V. E.: Analytic upscaling of local microphysics parameterizations, Part II: Simulations, *Quart. J. Royal Met. Soc.*, 139, 58–69, 2013.
- Guo, H., Golaz, J.-C., Donner, L. J., Ginoux, P., and Hemler, R. S.: Multivariate probability density functions with dynamics in the GFDL atmospheric general circulation model: Global tests, *Journal of Climate*, 27, 2087–2108, 2014.

- 695 Guo, H., Golaz, J.-C., Donner, L., Wyman, B., Zhao, M., and Ginoux, P.: CLUBB as a unified cloud parameterization: opportunities and challenges, *Geophysical Research Letters*, doi:10.1002/2015GL063672, 2015.
- Halloway, C. E. and Neelin, J. D.: Moisture vertical structure, column water vapor, and tropical deep convection, *J. Atmos. Sci.*, pp. 1665–1683, 2009.
- Hohenegger, C. and Bretherton, C. S.: Simulating deep convection with a shallow convection scheme, *Atmos. Chem. Phys.*, 11, 10 389–10 406, doi:10.5194/acp-11-10389-2011, 2011.
- 700 Iacono, M. J., Delamere, J. S., Mlawer, E. J., Shephard, M. W., Clough, S. A., and Collins, W. D.: Radiative forcing by long-lived greenhouse gases: Calculations with the AER radiative transfer models, *J. Geophys. Res.*, 113, doi:10.1029/2008JD009944, 2008.
- Jakob, C. and Klein, S. A.: The role of vertically varying cloud fraction in the parameterization of microphysical processes in the ECMWF model, *Quart. J. Roy. Meteor. Soc.*, 125, 941–965, 1999.
- 705 Jess, S., Spichtinger, P., and Lohmann, U.: A statistical subgrid-scale algorithm for precipitation formation in stratiform clouds in the ECHAM5 single column model, *Atmos. Chem. Phys. Discuss.*, 11, 9335–9374, 2011.
- Kain, J. S.: The Kain–Fritsch Convective Parameterization: An Update, *J. Appl. Meteor.*, 43, 170–181, 2004.
- 710 Khairoutdinov, M. and Randall, D. A.: A cloud resolving model as a cloud parameterization in the NCAR Community Climate System Model: Preliminary results, *Geophys. Res. Lett.*, 28, 3617–3620, 2001.
- Khairoutdinov, M., DeMott, C., and Randall, D. A.: Evaluation of the Simulated Interannual and Subseasonal Variability in an AMIP-Style Simulation Using the CSU Multiscale Modeling Framework, *J. Climate*, 21, 413–431, 2008.
- 715 Kim, D., Sperber, K., Stern, W., Waliser, D., Kang, I.-S., Maloney, E., Wang, W., Weickmann, K., Benedict, J., Khairoutdinov, M., Lee, M.-I., Neale, R., Suarez, M., Thayer-Calder, K., and Zhang, G.: Application of MJO simulation diagnostics to climate models, *J. of Cli.*, 22, 6413–6436, 2009.
- Kim, D., Xavier, P., Maloney, E., Wheeler, M., Waliser, D., Sperber, K., Hendon, H., Zhang, C., Neale, R., Hwang, Y.-T., and Liu, H.: Process-Oriented MJO Simulation Diagnostic: Moisture Sensitivity of Simulated
- 720 Convection, *J. of Cli.*, 27, 5379–5395, 2014.
- Lappen, C.-L. and Randall, D. A.: Towards a unified parameterization of the boundary layer and moist convection. Part I: A new type of mass-flux model, *J. Atmos. Sci.*, 58, 2021–2036, 2001.
- Larson, V. E. and Golaz, J.-C.: Using probability density functions to derive consistent closure relationships among higher-order moments, *Mon. Wea. Rev.*, 133, 1023–1042, 2005.
- 725 Larson, V. E. and Griffin, B. M.: Analytic upscaling of local microphysics parameterizations, Part I: Derivation, *Quart. J. Royal Met. Soc.*, 139, 46–57, 2013.
- Larson, V. E. and Schanen, D. P.: The Subgrid Importance Latin Hypercube Sampler (SILHS): a multivariate subcolumn generator, *Geosci. Model Dev.*, 6, 1813–1829, doi:10.5194/gmdd-6-1813-2013, 2013.
- Larson, V. E., Wood, R., Field, P. R., Golaz, J.-C., Vonder Haar, T. H., and Cotton, W. R.: Systematic biases in the microphysics and thermodynamics of numerical models that ignore subgrid-scale variability, *J. Atmos. Sci.*, 58, 1117–1128, 2001.
- 730 Larson, V. E., Golaz, J.-C., and Cotton, W. R.: Small-scale and mesoscale variability in cloudy boundary layers: Joint probability density functions, *J. Atmos. Sci.*, 59, 3519–3539, 2002.

- Larson, V. E., Golaz, J.-C., Jiang, H., and Cotton, W. R.: Supplying Local Microphysics Parameterizations with
 735 Information about Subgrid Variability: Latin Hypercube Sampling, *J. Atmos. Sci.*, 62, 4010–4026, 2005.
- Larson, V. E., Schanen, D. P., Wang, M., Ovchinnikov, M., and Ghan, S.: PDF parameterization of boundary
 layer clouds in models with horizontal grid spacings from 2 to 16 km, *Mon. Wea. Rev.*, 140, 285–306, 2012.
- Lebo, Z. J., Williams, C. R., Feingold, G., and Larson, V. E.: Parameterization of rain rate variability for large-
 scale models, submitted to *J. Appl. Meteor. Climatol.*, 2015.
- 740 Lewellen, W. S. and Yoh, S.: Binormal model of ensemble partial cloudiness, *J. Atmos. Sci.*, 50, 1228–1237,
 1993.
- Lin, J.-L., Lee, M.-I., Kim, D., Kang, I.-S., and Frierson, D. M.: The impacts of convective parameterization
 and moisture triggering on AGCM-simulated convectively coupled equatorial waves, *Journal of Climate*, 21,
 883–909, 2008.
- 745 Liu, X., Easter, R. C., Ghan, S. J., Zaveri, R., Rasch, P., Shi, X., Lamarque, J.-F., Gettelman, A., Morrison, H.,
 Vitt, F., Conley, A., Park, S., Neale, R., Hannay, C., Ekman, A. M. L., Hess, P., Mahowald, N., Collins, W., Iacono,
 M. J., Bretherton, C. S., Flanner, M. G., and Mitchell, D.: Toward a minimal representation of aerosols
 in climate models: description and evaluation in the Community Atmosphere Model CAM5, *Geosci. Model
 Dev.*, 5, 709–739, doi:10.5194/gmd-5-709-2012, <http://www.geosci-model-dev.net/5/709/2012/>, 2012.
- 750 Manton, M. J. and Cotton, W. R.: Formulation of approximate equations for modeling moist deep convection
 on the mesoscale, Atmospheric science paper no. 266, Colorado State University, Fort Collins, CO, 1977.
- Mellor, G. L.: The Gaussian cloud model relations, *J. Atmos. Sci.*, 34, 356–358, 1977.
- Moncrieff, M. W.: Organized convective systems: Archetypal dynamical models, mass and momentum flux
 theory, and parametrization, *Quart. J. Roy. Meteor. Soc.*, 118, 819–850, 1992.
- 755 Moncrieff, M. W. and Liu, C.: Representing convective organization in prediction models by a hybrid strategy,
J. Atmos. Sci., 63, 3404–3420, 2006.
- Morrison, H. and Gettelman, A.: A new two-moment bulk stratiform cloud microphysics scheme in the Com-
 munity Atmosphere Model, Version 3 (CAM3). Part I: Description and numerical tests, *J. Climate.*, 21,
 3642–3659, 2008.
- 760 Nakanishi, M. and Niino, H.: An improved Mellor–Yamada level-3 model with condensation physics: Its design
 and verification, *Bound.-layer Meteor.*, 112, 1–31, 2004.
- Neale, R. B., Gettelman, A., Park, S., Chen, C.-C., Lauritzen, P. H., Williamson, D. L., Conley, A. J., Kin-
 nison, D., Marsh, D., Smith, A. K., Vitt, F., Garcia, R., Lamarque, J.-F., Mills, M., Tilmes, S., Morrison,
 H., Cameron-Smith, P., Collins, W. D., Iacono, M. J., Easter, R. C., Ghan, S. J., Liu, X., Rasch, P. J., and
 765 Taylor, M. A.: Description of the NCAR Community Atmosphere Model (CAM5.0), Tech. Rep. NCAR/TN-
 486+STR, National Center for Atmospheric Research, Boulder, CO, USA, 2012.
- Neggers, R. A. J.: A Dual Mass Flux Framework for Boundary Layer Convection. Part II: Clouds, *J. Atmos.
 Sci.*, 66, 1489–1506, 2009.
- Neggers, R. A. J., Köhler, M., and Beljaars, A. C. M.: A Dual Mass Flux Framework for Boundary Layer
 770 Convection. Part I: Transport, *J. Atmos. Sci.*, 66, 1465–1488, 2009.
- Park, S.: A unified convection scheme (UNICON). Part I: Formulation, *Journal of the Atmospheric Sciences*,
 71, 3902–3930, 2014a.

- Park, S.: A unified convection scheme (UNICON). Part II: Simulation, *Journal of the Atmospheric Sciences*, 71, 3931–3973, 2014b.
- 775 Park, S. and Bretherton, C. S.: The University of Washington Shallow Convection and Moist Turbulence Schemes and Their Impact on Climate Simulations with the Community Atmosphere Model, *J. Climate*, 22, 3449–3469, 2009.
- Pincus, R. and Klein, S. A.: Unresolved spatial variability and microphysical process rates in large-scale models, *J. Geophys. Res.*, 105, 27 059–27 065, 2000.
- 780 Pincus, R., Barker, H. W., and Morcrette, J.-J.: A fast, flexible, approximate technique for computing radiative transfer in inhomogeneous cloud fields, *J. Geophys. Res.*, 108, Art. No. 4376, doi: 10.1029/2002JD003322, 2003.
- Pincus, R., Hemler, R., and Klein, S. A.: Using stochastically-generated subcolumns to represent cloud structure in a large-scale model, *Mon. Wea. Rev.*, 134, 3644–3656, 2006.
- 785 Räisänen, P. and Barker, H. W.: Evaluation and optimization of sampling errors for the Monte Carlo Independent Column Approximation, *Quart. J. Roy. Meteor. Soc.*, 130, 2069–2085, 2004.
- Räisänen, P., Barker, H. W., Khairoutdinov, M. F., Li, J., and Randall, D. A.: Stochastic generation of subgrid-scale cloudy columns for large-scale models, *Quart. J. Roy. Meteor. Soc.*, 130, 2047–2067, 2004.
- Räisänen, P., Barker, H. W., and Cole, J. N. S.: The Monte Carlo Independent Column Approximation’s conditional random noise: Impact on simulated climate, *J. Climate*, 18, 4715–4730, doi:10.1175/JCLI3556.1, 2005.
- 790 Räisänen, P., Järvenoja, S., Järvinen, H., Giorgetta, M., Roeckner, E., Jylhä, K., and Ruosteenoja, K.: Tests of Monte Carlo Independent Column Approximation in the ECHAM5 Atmospheric GCM, *J. Climate*, 20, 4995–5011, doi:10.1175/JCLI4290.1, 2007.
- 795 Räisänen, P., Järvenoja, S., and Järvinen, H.: Noise due to the Monte Carlo independent-column approximation: short-term and long-term impacts in ECHAM5, *Quart. J. Roy. Meteor. Soc.*, 134, 481–495, 2008.
- Raut, E. K. and Larson, V. E.: A Flexible Importance Sampling Method for Integrating Subgrid Processes, submitted to *Geoscientific Model Development Discussions*, 2015.
- Siebesma, A. P., Soares, P. M. M., and Teixeira, J.: A Combined Eddy-Diffusivity Mass-Flux Approach for the Convective Boundary Layer, *J. Atmos. Sci.*, 64, 1230–1248, 2007.
- 800 Smith, R. N. B.: A scheme for predicting layer clouds and their water content in a general circulation model, *Quart. J. Roy. Meteor. Soc.*, 116, 435–460, 1990.
- Soares, P. M. M., Miranda, P. M. A., Siebesma, A. P., and Teixeira, J.: An eddy-diffusivity/mass-flux parametrization for dry and shallow cumulus convection, *Quart. J. Roy. Meteor. Soc.*, 130, 3365–3383, 2004.
- 805 Sommeria, G. and Deardorff, J. W.: Subgrid-scale condensation in models of nonprecipitating clouds, *J. Atmos. Sci.*, 34, 344–355, 1977.
- Stephens, G. L., Li, J., Wild, M., Clayson, C. A., Loeb, N., Kato, S., L’Ecuyer, T., Jr., P. W. S., Lebsock, M., and Andrews, T.: An update on Earth’s energy balance in light of the latest global observations, *Nature Geoscience*, 5, 691–696, doi:10.1038/NGEO1580, 2012.
- 810 Storer, R. L., Griffin, B. M., Höft, J., Weber, J. K., Raut, E., Larson, V. E., Wang, M., and Rasch, P. J.: Parameterizing deep convection using the assumed probability density function method, *Geoscientific Model Development*, 8, 1–19, 2015.

- Sušelj, K., Teixeira, J., and Matheou, G.: Eddy diffusivity/mass flux and shallow cumulus boundary layer: An updraft PDF multiple mass flux scheme, *J. Atmos. Sci.*, 69, 1513–1533, 2012.
- 815 Sušelj, K., Teixeira, J., and Chung, D.: A unified model for moist convective boundary layers based on a stochastic eddy-diffusivity/mass-flux parameterization, *J. Atmos. Sci.*, 70, 1929–1953, 2013.
- Sušelj, K., Hogan, T. F., and Teixeira, J.: Implementation of a stochastic eddy-diffusivity/mass-flux parameterization into the Navy Global Environmental Model, *Wea. Forecasting*, 29, 1374–1390, 2014.
- Taylor, K. E.: Summarizing multiple aspects of model performance in a single diagram, *Journal of Geophysical Research: Atmospheres*, 106, 7183–7192, doi:10.1029/2000JD900719, <http://dx.doi.org/10.1029/2000JD900719>, 2001.
- 820 Thayer-Calder, K. and Randall, D.: The Role of Convective Moistening in the Madden-Julian Oscillation, *J. Atmos. Sci.*, 66, 3297–3312, doi:10.1175/2009JAS3081.1, 2009.
- Tompkins, A. M.: A prognostic parameterization for the subgrid-scale variability of water vapor and clouds in large-scale models and its use to diagnose cloud cover, *J. Atmos. Sci.*, 59, 1917–1942, 2002.
- 825 Tonttila, J., Räisänen, P., and Järvinen, H.: Monte Carlo-based subgrid parameterization of vertical velocity and stratiform cloud microphysics in ECHAM5.5-HAM2, *Atmospheric Chemistry and Physics*, 13, 7551–7565, doi:10.5194/acp-13-7551-2013, 2013.
- Tonttila, J., Järvinen, H., and Räisänen, P.: Explicit representation of subgrid variability in cloud microphysics yields weaker aerosol indirect effect in the ECHAM5-HAM2 climate model, *Atmos. Chem. and Phys.*, 15, 703–714, doi:10.5194/acp-15-703-2015, 2015.
- 830 Wheeler, M. and Kiladis, G. N.: Convectively Coupled Equatorial Waves: Analysis of Clouds and Temperature in the Wavenumber-Frequency Domain, *J. of Atmos. Sci.*, 56, 374–399, 1999.
- Wu, C.-M., Stevens, B., and Arakawa, A.: What controls the transition from shallow to deep convection?, *J. Atmos. Sci.*, 66, 1793–1806, 2009.
- 835 Xavier, P. K.: Intraseasonal convective moistening in CMIP3 models, *J. Climate*, 25, 2569–2577, 2012.
- Yano, J.-i., Redelsperger, J.-l., Bechtold, P., and Guichard, F.: Mode decomposition as a methodology for developing convective-scale representations in global models, *Quart. J. Roy. Meteor. Soc.*, 131, 2313–2336, 2005.
- 840 Zhang, G. J. and McFarlane, N. A.: Sensitivity of climate simulations to the parameterization of cumulus convection in the Canadian Climate Centre general circulation model, *Atmosphere Ocean*, 33, 407–446, 1995.
- Zhang, M. and Bretherton, C.: Mechanisms of Low Cloud–Climate Feedback in Idealized Single-Column Simulations with the Community Atmospheric Model, Version 3 (CAM3), *J. Climate*, 21, 4859–4878, 2008.

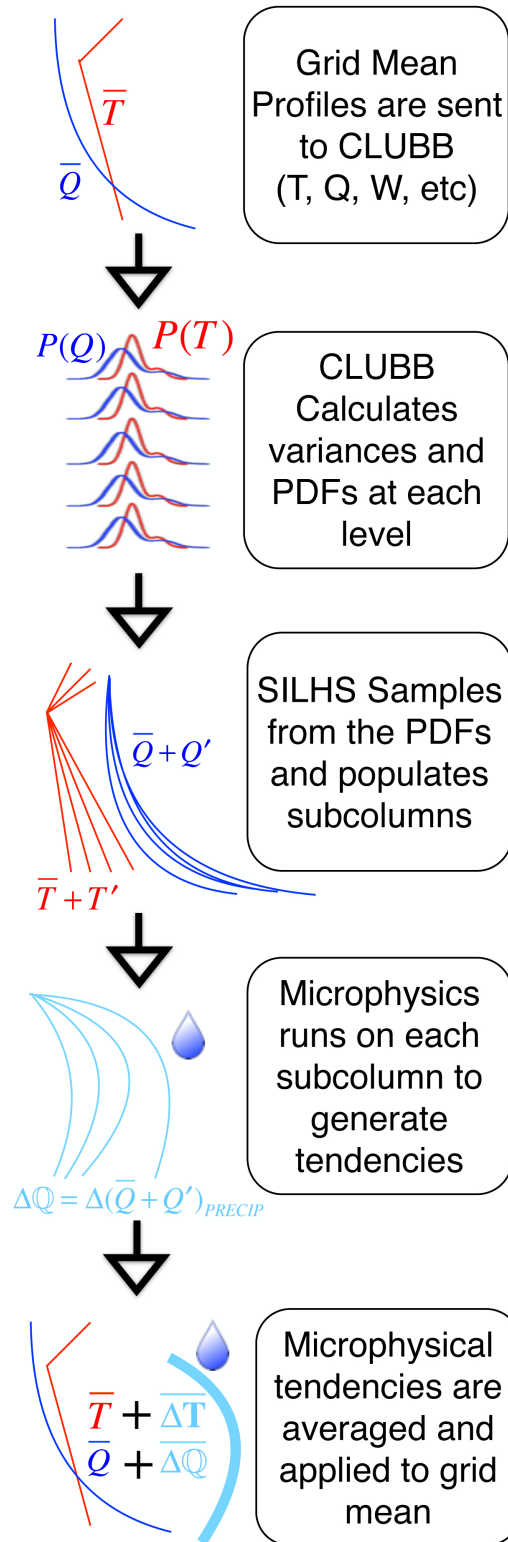


Figure 1. The sequence of calculations in CAM-CLUBB-SILHS. Red lines represent temperature profiles and dark blue lines represent moisture profiles, as an example. Light blue lines represent figurative microphysical tendencies, for both temperature and moisture. For details on the SILHS and subcolumn methodology, see Section 2.

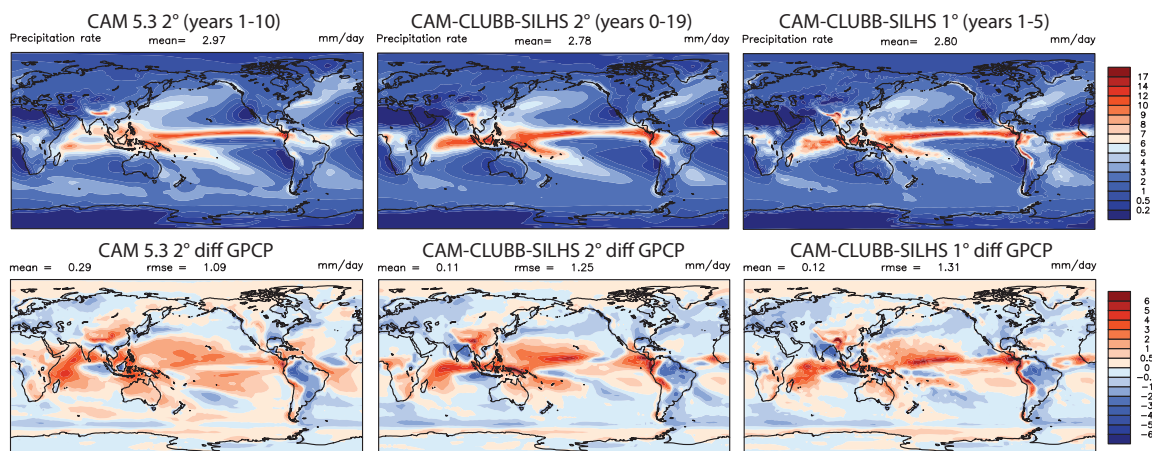


Figure 2. Total surface precipitation rate for CAM 5.3 (left), CAM-CLUBB-SILHS 2 degree (center), and CAM-CLUBB-SILHS 1 degree (right). The difference from GPCP observations of precipitation rate is shown in the second row. CAM-CLUBB-SILHS has more intense precipitation, but less of a double ITCZ than CAM 5.3.

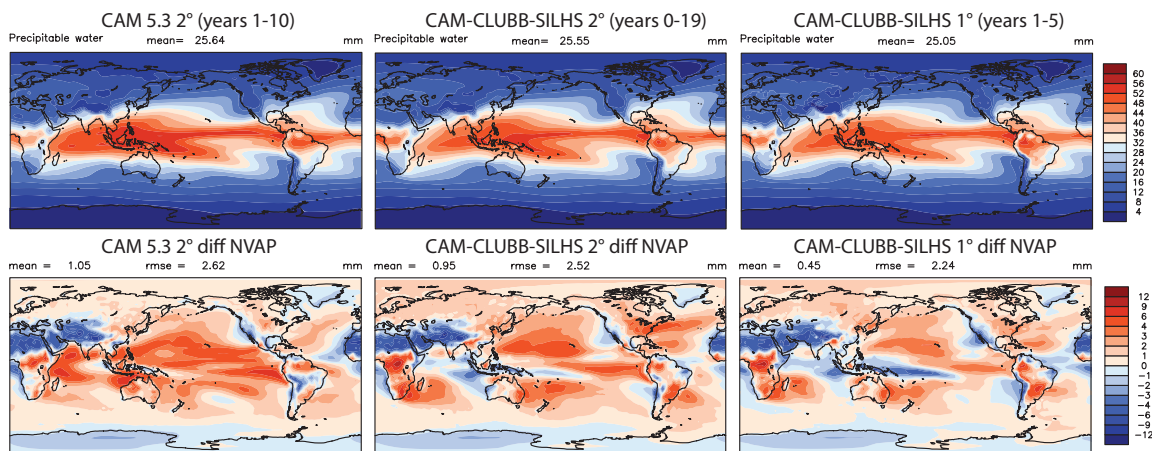


Figure 3. Total column water vapor field for CAM 5.3 (left), CAM-CLUBB-SILHS 2 degree (center), and CAM-CLUBB-SILHS 1 degree (right). The difference from National Aeronautics and Space Administration (NASA) Water Vapor Project (NVAP) satellite observations (model - obs) is shown in the second row. CAM-CLUBB-SILHS reduces the overall moist bias seen in CAM 5.3.

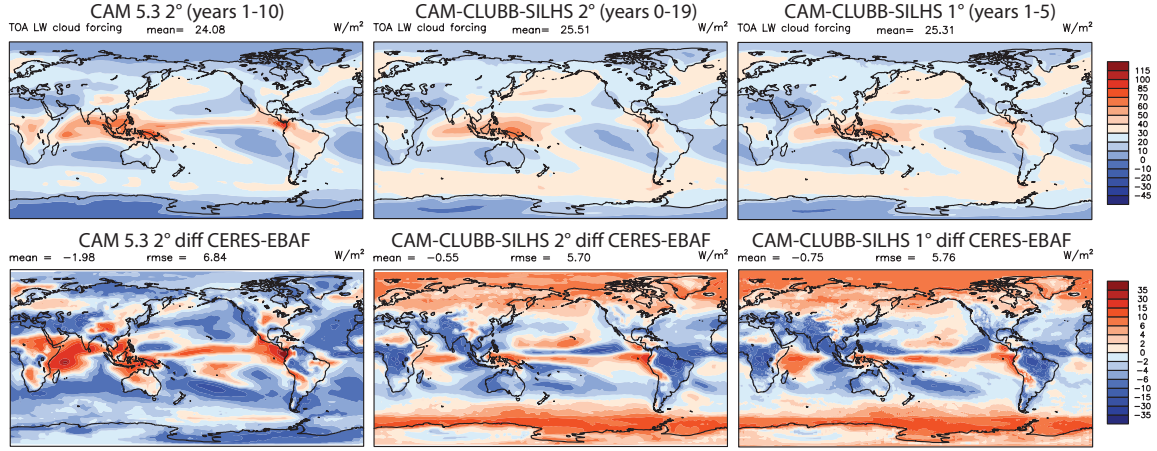


Figure 4. Top of the atmosphere long wave cloud forcing (LWCF) for CAM 5.3 (left), CAM-CLUBB-SILHS 2 degree (center), and CAM-CLUBB-SILHS 1 degree (right). The difference from Clouds and Earth's Radiant Energy Systems (CERES) Energy Balanced and Filled (EBAF) observations of LWCF (model-obs) is shown in the second row. CAM-CLUBB-SILHS has a slightly lower global error in LWCF than CAM 5.3 due to an increase in cloud forcing in the mid-latitudes and polar regions.

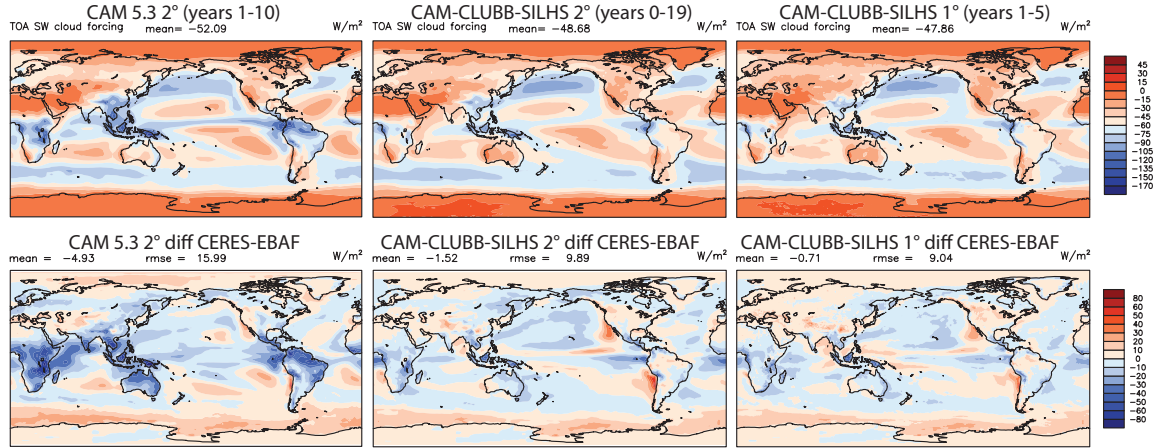


Figure 5. Top of the atmosphere short wave cloud forcing (SWCF) for CAM 5.3 (left), CAM-CLUBB-SILHS 2 degree (center), and CAM-CLUBB-SILHS 1 degree (right). The difference from CERES-EBAF observations of SWCF is shown in the second row. CAM-CLUBB-SILHS reduces the SWCF low bias over tropical land regions seen in CAM 5.3.

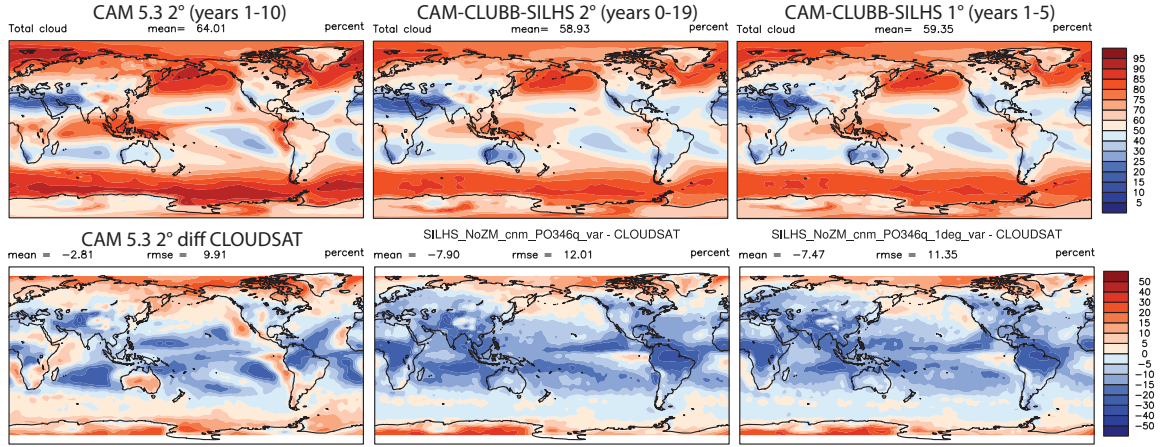


Figure 6. Total grid box cloud fraction for CAM 5.3 (left), CAM-CLUBB-SILHS 2 degree (center), and CAM-CLUBB-SILHS 1 degree (right). The difference from CLOUDSAT observations of total cloud fraction is shown in the second row. The global mean cloud fraction in CAM-CLUBB-SILHS is reduced by about 5% compared to the CAM 5.3 mean value.

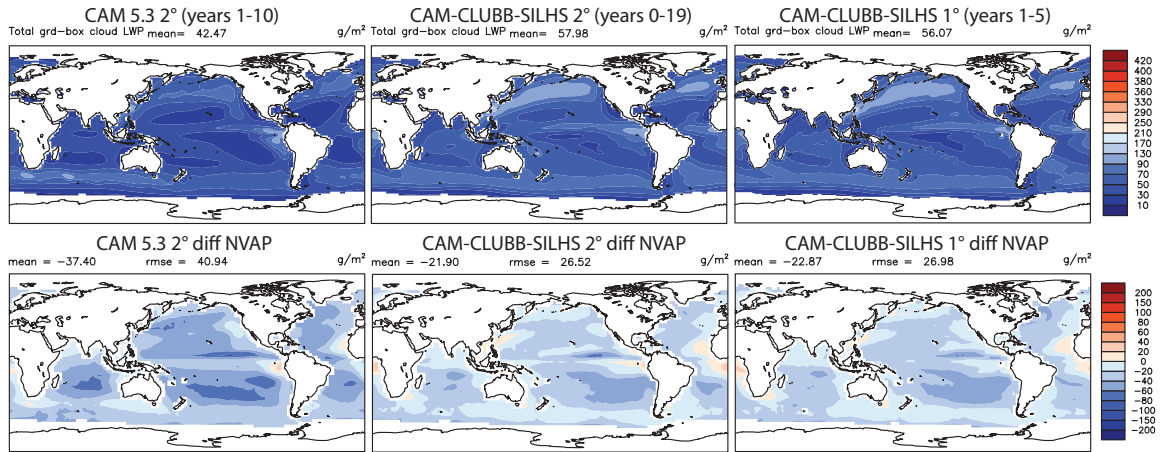


Figure 7. Total grid box liquid water path (LWP) for CAM 5.3 (left), CAM-CLUBB-SILHS 2 degree (center), and CAM-CLUBB-SILHS 1 degree (right). The difference from NVAP observations of LWP is shown in the second row. The global mean LWP in CAM-CLUBB-SILHS is about 35% higher than that of CAM 5.3.

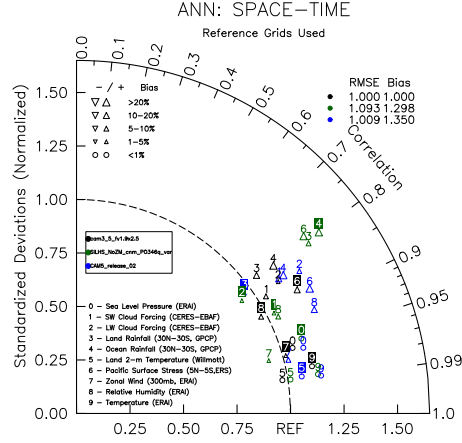


Figure 8. Taylor diagram with metrics for CAM 3.5 (black), CAM 5.3 (blue), and 2-degree CAM-CLUBB-SILHS (green). CAM-CLUBB-SILHS is competitive for all metrics except ocean and land rainfall, and Pacific surface stress.

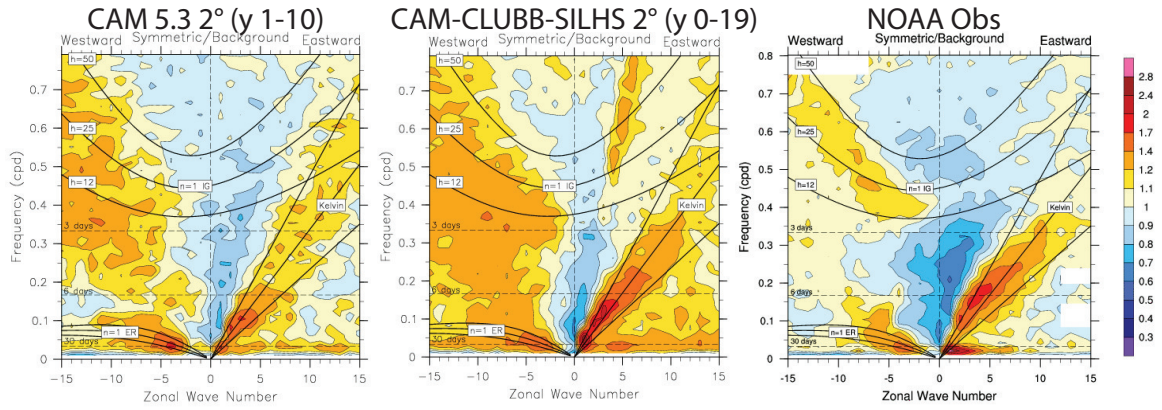


Figure 9. OLR power divided by the background spectra for various wavenumbers and frequencies in the tropics for CAM 5.3 (left), CAM-CLUBB-SILHS (center), and NOAA OLR observations (right). CAM-CLUBB-SILHS has stronger MJO signal, and a stronger signal for Kelvin waves, than CAM 5.3

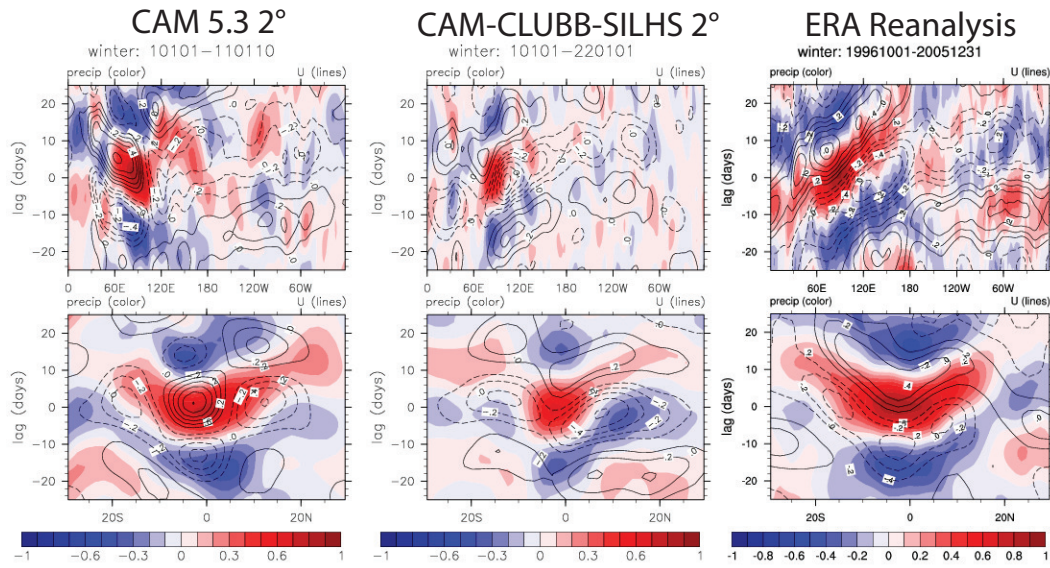


Figure 10. Lag-Longitude plots of winter MJO wave activity (top row), and Lag-Latitude plots of winter MJO wave activity (bottom row) for CAM 5.3 (left column), CAM-CLUBB-SILHS (center column), and ERA Reanalysis (right column). Precipitation is denoted by colors, zonal wind by lines. The signal in CAM-CLUBB-SILHS is weaker than observations, but the wave is moving eastward, rather than westward as in CAM 5.3.

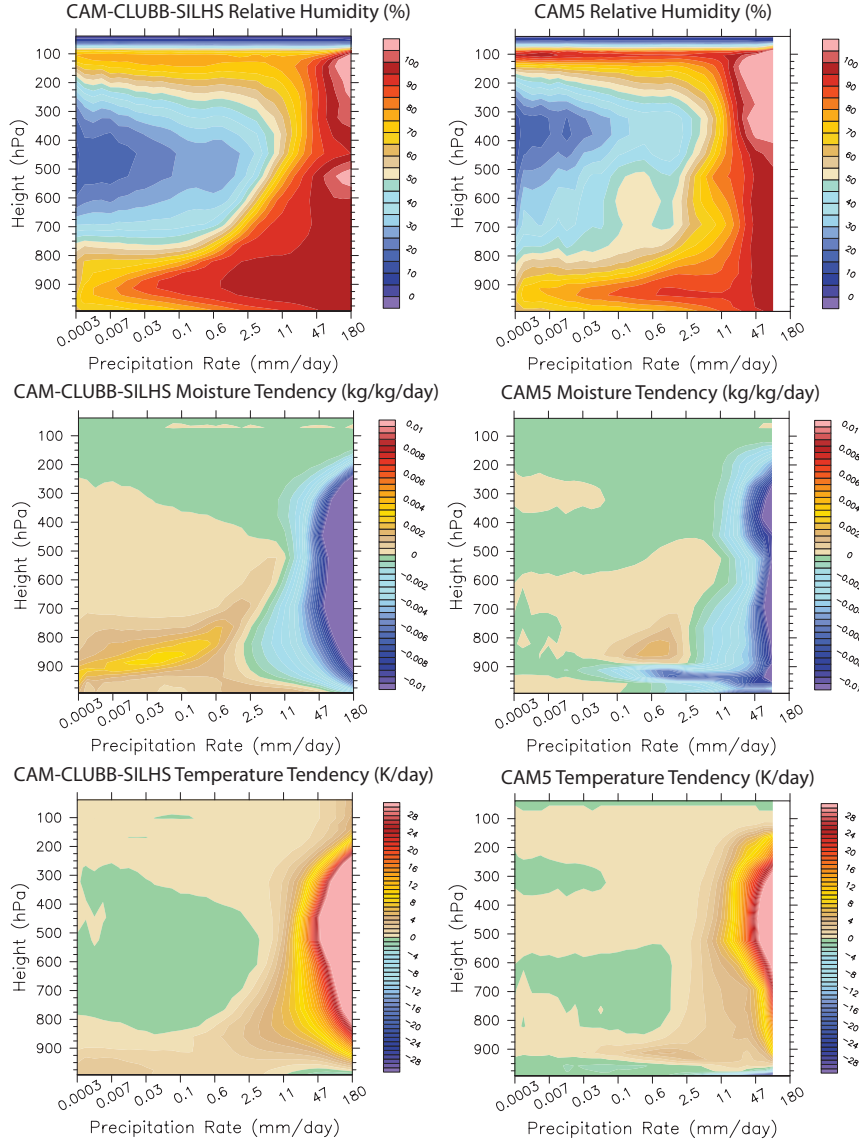


Figure 11. Daily average profiles of fields per daily average value of precipitation for the region between latitudes 15N and 15S and longitudes 60E to 180E over one year. Relative humidity for CAM-CLUBB-SILHS (top left) and CAM5 (top right), total physics moisture tendencies for CAM-CLUBB-SILHS (middle left) and CAM5 (middle right), and total physics temperature tendencies for CAM-CLUBB-SILHS (bottom left) and CAM5 (bottom right) are shown. Because CAM-CLUBB-SILHS is a unified parameterization, there is a smoother transition from light to intense precipitation values for all fields.

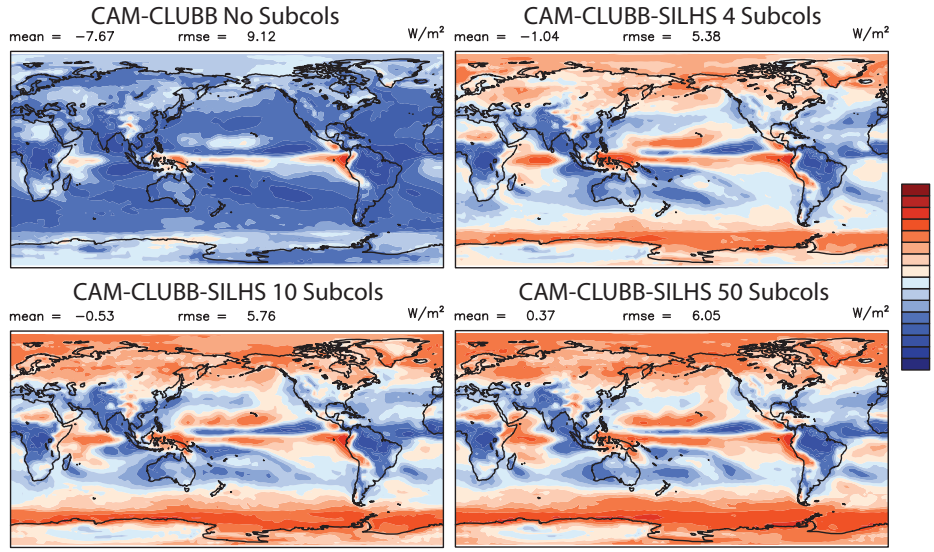


Figure 12. LWCF difference from CERES-EBAF observations for five years of simulation without subcolumns at all (top left), 4 subcolumns (top right), 10 subcolumns (bottom left), and 50 subcolumns (bottom right). Without subcolumns, the LWCF has a severe low bias. The simulation with 4 subcolumns has the lowest global error, and very little changes between the simulations with 10 and 50 subcolumns.

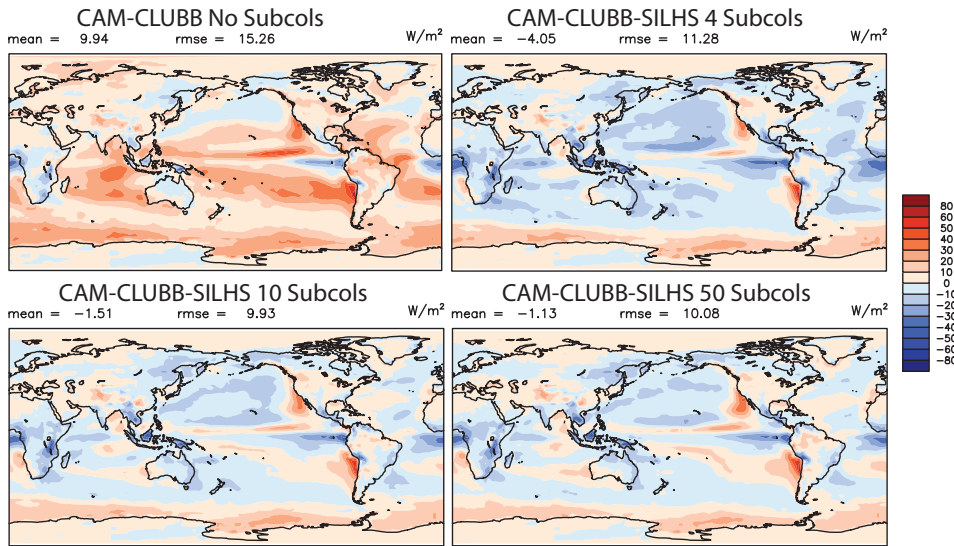


Figure 13. Simulated SWCF minus CERES-EBAF observations for five years of simulation without subcolumns at all (top left), 4 subcolumns (top right), 10 subcolumns (bottom left), and 50 subcolumns (bottom right). Without subcolumns, the clouds are too dim. The simulation with 4 subcolumns has brighter clouds than observed, and the simulations with 10 and 50 subcolumns differ little from each other.

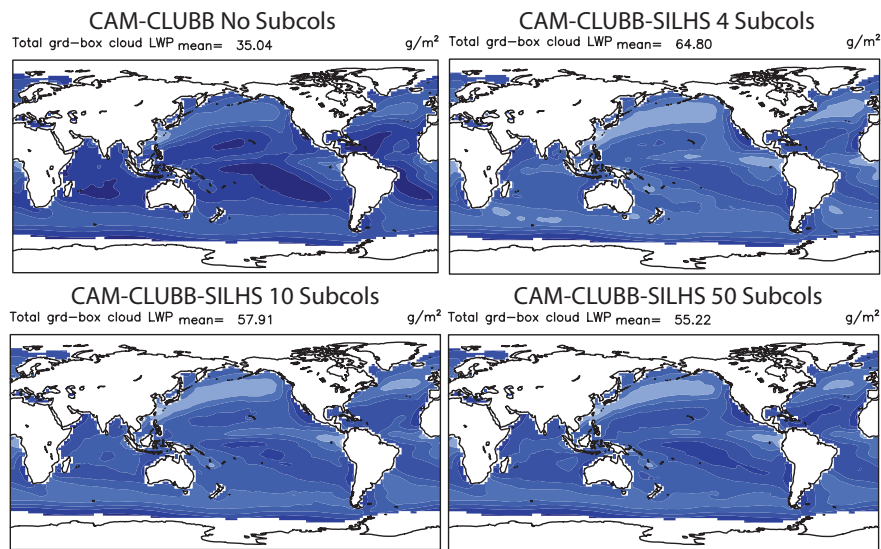


Figure 14. LWP for five years of simulation without subcolumns at all (top left), 4 subcolumns (top right), 10 subcolumns (bottom left), and 50 subcolumns (bottom right). Without subcolumns, the model has little cloud liquid water. The simulation with 4 subcolumns has a large amount of cloud liquid, which moderates in the 10 and 50 subcolumn simulations.

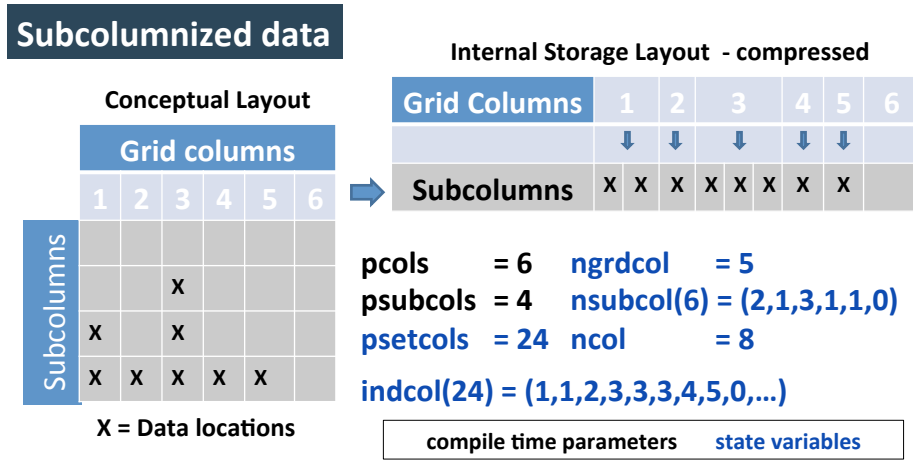


Figure A1. Schematic for CAM's subcolumn software framework. The number of subcolumns varies by grid column, as shown in the conceptual layout (left). Internally, the subcolumns are stored in a compressed layout (right). The information on per-chunk linkages is stored in a series of software parameters, some of which can be set by the user (black) and others of which are internally calculated (blue). *pcols* is the maximum number of grid columns, *psubcols* is the maximum number of subcolumns, *psetcols* is the maximum number of all columns ($= pcols * psubcols$), *ngrdcol* is the actual number of grid columns that contain data, *nsubcol(pcols)* is the number of subcolumns in each grid column with data, *ncol* is the total number of all subcolumns with data, and *indcol(psetcols)* is the grid index for each subcolumn, which is used for mapping subcolumns back to grid columns.

Table 1. Physical parameterizations in CAM 5.3 and CAM-CLUBB-SILHS

Physics	CAM 5.3	CAM-CLUBB-SILHS
Deep Convection	Zhang and McFarlane (1995)	CLUBB-SILHS
Shallow Convection	Park and Bretherton (2009)	CLUBB-SILHS
Boundary Layer	Bretherton and Park (2009)	CLUBB-SILHS
Cloud Macrophysics	Park (Neale et al., 2012)	CLUBB-SILHS
Cloud Microphysics	Morrison and Gettelman (2008)	Morrison and Gettelman (2008)
Radiation	Rapid Radiative Transfer Model for GCMs (RRTMG); Iacono et al. (2008)	RRTMG; Iacono et al. (2008)
Aerosols	Liu et al. (2012)	Liu et al. (2012)

Table 2. Computational cost of CAM 5.3 and CAM-CLUBB-SILHS simulations.

Simulation	Number of Processors	Years/Computer-day	Percent Increase Over CAM5.3
CAM 5.3	256	20.2	–
0 sc	256	12.4	63%
4 sc	256	10.7	89%
10 sc	256	9.2	120%
50 sc	256	4.6	440%

Table 3. Information about observational datasets used for comparison in this paper. More information about each of these can be found on the website for the National Center for Atmospheric Research (NCAR) Climate Data Guide at <https://climatedataguide.ucar.edu/>.

Data Set	Acronym	Number of Years	Fields Used
National Aeronautics and Space Administration (NASA) Water Vapor Project	NVAP	14 (1988-2001)	Total column water vapor and cloud liquid water
Global Precipitation Climatology Project	GPCP	30 (1979-2009)	Total Precipitation Rate
Clouds and Earth's Radiant Energy Systems - Energy Balanced and Filled	CERES-EBAF	13 (2000-2013)	TOA longwave flux, shortwave flux, longwave cloud forcing, shortwave cloud forcing and radiation imbalance.
NASA CloudSat	CloudSat	4 (2006-2010)	Total cloud fraction
National Oceanic and Atmospheric Administration Polar-orbiting Operational Environmental Satellites	NOAA POES	21 (1979-2000)	TOA (outgoing) longwave radiation
European Centre for Medium-Range Weather Forecasts Reanalysis - Interim	ERA-Interim	9 (1996-2005)	Precipitation and U 850 winds
National Centers for Environmental Prediction Reanalysis	NCEP Reanalysis (R1)	19 (1981-2000)	200hPa velocity potential

Table 4. Globally averaged top of the atmosphere (TOA) radiation fields, and the top of model (TOM) radiation imbalance for various configurations of CAM-CLUBB-SILHS. Estimates of observational uncertainty are from Stephens et al. (2012). Values are in units of W m^{-2} .

Simulation	Length	Net solar flux	Upward longwave flux	Longwave Cloud Forcing	Shortwave Cloud Forcing	TOM Imbalance
Observations (CERES-EBAF)	–	240.5 ± 2.0	239.7 ± 3.3	26.1 ± 4.0	-47.1 ± 3.0	–
CAM 5.3 2 degree	10 years	239.2	235.0	24.1	-52.1	2.118
CAM-CLUBB-SILHS 2 degree	20 years	241.9	236.4	25.5	-48.7	3.510
CAM-CLUBB-SILHS 1 degree	5 years	242.5	237.4	25.3	-47.9	3.001
CAM-CLUBB-SILHS No Subcols	5 years	254.1	243.4	18.4	-37.2	8.648
CAM-CLUBB-SILHS 4 Subcols	5 years	239.1	236.5	25.0	-51.2	0.520
CAM-CLUBB-SILHS 10 Subcols	5 years	241.9	236.3	25.5	-48.7	3.580
CAM-CLUBB-SILHS 50 Subcols	5 years	242.4	235.4	26.4	-48.3	4.982